Spin-polarized tunnel current in magnetic-layer systems and its relation to the interlayer exchange interaction

C. Heide and R. J. Elliott
University of Oxford, Department of Physics, Theoretical Physics, 1 Keble Road, Oxford OX1 3NP, United Kingdom

Ned S. Wingreen
NEC Research Institute, 4 Independence Way, Princeton, New Jersey 08540

(Received 24 July 1998)

The spin-polarized tunnel current and its connection to the interlayer exchange interaction is studied in ferromagnet-insulator-ferromagnet thin-film planar junctions out of equilibrium. Building on the nonequilibrium Keldysh formalism, it is possible to systematically include a contact interaction between localized spins and conduction electrons and extend previous treatments on spin currents and exchange interaction. In particular, a Landauer-type formula is derived for the spin current that explains the result found earlier [Schwabe, Wingreen, and Elliott, Phys. Rev. B **54**, 12 953 (1996)] that the exchange interaction between the ferromagnetic slabs increases in proportion to the slab width. Furthermore, switching is shown to occur between parallel and antiparallel coupling of the slabs for different applied biases under feasible experimental conditions. [S0163-1829(99)08705-6]

I. INTRODUCTION

The discovery of antiferromagnetic coupling in Fe/Cr superlattices by Grünberg *et al.*[1] has led to a renewed interest in magnetic layer systems, partly due to the possibility of applying these structures as magnetoresistive sensors, for instance, in magnetic reading heads[2] or as magnetoresistance random access memories.[3] Prior to this, Julliere already experimented on tunneling in ferromagnet-insulator-ferromagnet trilayer thin-film planar junctions that showed the interesting magnetoresistive effect that tunneling depends on the angle between the moments of the ferromagnets.[4] However, the tunnel magnetoresistance was not very large in the early stages of experiments.[5–7] Only recently considerable tunnel magnetoresistance was observed by several groups in trilayer structures[8–10] that led to suggestions that spin-dependent tunnel junctions offer another opportunity for building random access nonvolatile memories with high impedance and low interlayer coupling.[11]

The work of Tedrow and Meservey, who measured the tunnel conductance of superconductor-insulator-ferromagnet films, is crucial in understanding magnetic trilayer junctions. They showed that tunneling out of a ferromagnetic electrode is spin polarized.[12] Using this result, Julliere performed his pioneering work on tunneling between two ferromagnets in a Fe/Ge/Co trilayer where for zero bias he observed anomalies with different resistances for parallel and antiparallel alignment of the magnetizations of the ferromagnets. He put forward a simple model that explains this magnetoresistive effect in terms of the spin-dependent density of states at the Fermi level in each ferromagnet. The model was extended by Slonczewski who matched wave functions for spin-up and spin-down conduction electrons between magnetic and insulating layers, where the insulator was approximated by a square barrier potential of low transmission.[13] According to his theory, spin tunneling across the interfaces is significantly influenced by the barrier height. Both pictures roughly predict the qualitative behavior of the magnetoresistance in ferromagnetic tunnel junctions. However, they leave open details in the interpretation of the decrease in magnetoresistance for increasing bias across the junction.

Another aspect of spin-dependent transport was pointed out by Aronov who suggested that spin injection arises when a current flows from a ferromagnetic metal into a nonmagnetic one.[14] Later, Johnson and Silsbee could verify Aronov's theory with their spin injection experiment[15] and introduced the concept of interfacial charge-spin coupling.[16]

Spin injection and tunnel magnetoresistance are different aspects of spin-dependent transport. To analyze both aspects, we derive in this paper a Landauer-type formula for the spin-polarized current of the biased junction based on a model that takes the spin dependence of the band structure into account similar to the treatment of Slonczewski.[13] The model builds on the nonequilibrium theories for tunnel systems by Caroli[17–20] and Feuchtwang.[21–23]

Related to spin-dependent transport is the exchange interaction between ferromagnetic films across a spacer. Testing a considerable range of thicknesses of metallic spacers, Parkin *et al.* observed oscillations in the giant magnetoresistance.[24] Referring to Yafet, who calculated the range function of the interaction between two magnetic monolayers,[25] they argued that these oscillations mirror the changes between ferromagnetic and antiferromagnetic coupling of the layers. Unlike the semiclassical model by Julliere for spin currents, the exchange coupling is a true quantum-mechanical effect. The interaction between the magnetic moments in the ferromagnets is mediated by polarized conduction electrons, also known as the Ruderman-Kittel-Kasuya-Yosida (RKKY) interaction. This approach has been extended by Baltensperger and Helman[26] as well as Bruno and Chappert[27] to calculate a more realistic model for the exchange coupling between ferromagnetic layers across a metallic spacer by direct application of the RKKY theory to the specific geometries of the system. The coupling arises then from the polarization of

magnetic carriers in the spacer metal analogous to the usual RKKY theory. Edwards *et al.* developed a different approach.[28,29] They argued that oscillations in the coupling result from quantum interference effects of spin-dependent electron waves inside the well formed between the ferromagnetic layers. This intuitive picture of the interlayer coupling leads to the comparison of a magnetic double layer with an optical resonator, like a Fabry-Pérot interferometer.[30,31] The RKKY-like interaction was shown to be the limit to the quantum-well model for weak exchange interaction inside the ferromagnets by d'Albuquerque e Castro *et al.*[32] and later by Bruno.[33] Apart from oscillations due to the metallic spacer thickness, oscillations were observed which change with the thickness of the ferromagnets[34] as predicted by numerical calculations of Barnas.[35] Bruno gave an intuitive explanation of this effect[31] by writing the interlayer exchange coupling in terms of reflection and transmission coefficients.

Whereas most of the work has been done on metallic spacer materials, ferromagnetic and antiferromagnetic coupling has also been found across semiconductor interlayers by Toscano *et al.*[36] and Fullerton *et al.*[37] This coupling is much weaker than the one across metallic spacers as long as the system is in equilibrium. Recently, Schwabe, Wingreen, and Elliott investigated the interaction between conduction electrons and magnetic moments of the ferromagnets in a trilayer junction.[38] They calculated the exchange interaction between the ferromagnets that is also of the RKKY type. The coupling depends not only on the height of the barrier but also on the thickness of the insulator and ferromagnets. Further, the presence of a nonequilibrium bias across the junction significantly alters the range of the coupling such that there is a component of the interaction energy between the ferromagnets proportional to their thickness and therefore it appears to act as an uniform magnetic field. To investigate the origins of this unexpected coupling behavior, we study another form of the spin-polarized tunnel current of the biased junction in a model that is analogous to that used for calculating the exchange interaction. Again, a Landauer-type formula is derived from the nonequilibrium theories for tunnel systems by Caroli and Feuchtwang that includes, in addition, a contact interaction between localized spins and conduction electrons.

The spin dependence in both Landauer-type formulas derives from different approximations to the *s*-*d* exchange Hamiltonian. The first model is a mean field approximation that relates to the treatments of Julliere,[4] Aronov,[14] Slonczewski[13] and, in particular, to that of Tsymbal and Pettifor.[39] It gives a good account of spin-dependent tunneling when ferromagnetism is strong and the layers not too thin. The second model is a perturbation treatment that is common to RKKY-like studies of the interlayer exchange interaction. This description is microscopically more satisfying and in particular takes the finite-size effects of the ferromagnets into account. We find that the spin current depends on spin-dependent scattering of conduction electrons at *d* electrons that are assumed to be localized. A nonequilibrium spin polarization is caused by the interference of incident spin-independent conduction electron waves and spin-dependent reflected waves. For both models we derive expressions for the spin current and the interlayer coupling where all quantities are expressed in terms of simple transmission and reflection amplitudes. They lead to the same results under the limiting conditions of semi-infinite ferromagnets and weak band splitting. Using parameters from recent experiments we calculate spin current and the interlayer exchange as a function of applied bias numerically.

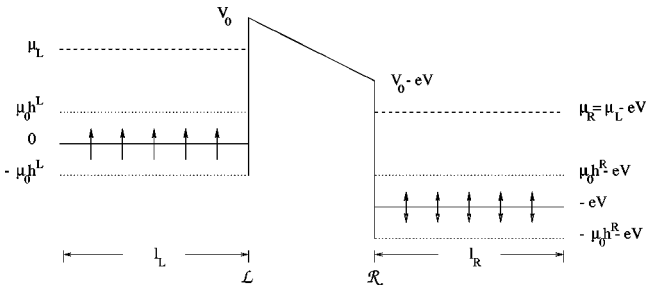

FIG. 1. Schematic representation of the ferromagnet-barrier-ferromagnet tunnel junction described in the text. The exchange interaction between the *d* electrons within a single ferromagnet causes a splitting of their band bottoms into two different spin subbands, indicated by the two punctuated lines on either side of the barrier. The *s*-*d* exchange coupling between the as-now localized regarded *d* electrons and itinerant *s* electrons spin polarizes a current driven through the system upon biasing the junction by *V*.

The remainder of the paper is structured as follows. Section II introduces the two models for ferromagnet-insulator-ferromagnet planar junctions out of equilibrium. Section III is devoted to a general comparison between spin-polarized tunnel current and interlayer exchange interaction. In Sec. IV the relevant definitions of the theories by Caroli *et al*. and Feuchtwang are introduced in order to derive expressions for the spin currents in Sec. V and exchange coupling in Sec. VI. Then, Sec. VII deals with numeric examples for both spin current and exchange interaction as functions of the applied voltage. Section VIII discusses the results of the presented theory for electron transfer in magnetic layered structures in relation to recent experiments. In conclusion, we summarize our results and point out further directions of studying magnetic trilayer systems in Sec. IX.

II. MODEL OF MAGNETIC-LAYER SYSTEM

The present paper addresses perpendicular transport and interlayer exchange interaction in a trilayer structure. As shown in Fig. 1, the trilayer structure consists of two planar ferromagnetic layers of length l_L and l_R, respectively, separated at the interfaces $\mathcal{L},\mathcal{R}$ by a nonmagnetic insulator of thickness $\mathcal{R}$-$\mathcal{L}$. This gives a quasi-one-dimensional model of a tunnel junction. Typical examples for the constituents of the ferromagnet-insulator-ferromagnet junction are Co, CoCr, CoFe, Fe, and NiFe for ferromagnets and Al_2O_3 and MgO for insulating nonmagnetic barriers.[8,9]

The magnetic order of band ferromagnets like Fe, Ni, and Co can to a large extent be traced back to electron correlation effects in relatively narrow $3d$ subbands, which only weakly hybridize with the $4s$ and $4p$ bands.[40] Due to the strong confinement of their atomic electron orbitals, we assume that the direct contribution of electrons in *d* subbands to transport across the barrier can be neglected. Although this is a gross simplification of the physical situation, it agrees with what was found by Tsymbal and Pettifor on the basis of band-

structure calculations.[39] They showed that the bonding between $3d$ metals and the oxide orbitals of the tunnel barrier must be very weak so that the d-electron contribution to tunneling is negligible regardless of their high density of states at the Fermi surface. The exchange coupling between the two ferromagnets across the barrier and the spin current are therefore assumed to originate from the interaction of the conduction electrons on the system of uncompensated magnetic moments of d electrons. This leads us to the approximation that neglects direct exchange interaction between d electrons and only takes the exchange interactions between s and d electrons into account such that the width of the d subbands is chosen to be zero and the effective mass of a d electron infinite, corresponding to complete localization.

The Hamiltonian of the system in Fig. 1 is written in terms of an unperturbed part H_0 and a part describing the exchange interaction $H_{s\text{-}d}$,

$$H = H_0 + H_{s\text{-}d}. \tag{1}$$

Due to the translational invariance of our model in the directions perpendicular to the current flow, the analysis is for now restricted to one dimension only and results will be extended later to three dimensions by Fourier transform. The unperturbed Hamiltonian with noninteracting conduction electrons with spin α in a single band is given by

$$H_0 = \sum_{\alpha} \int dx\, \Psi_{\alpha}^{\dagger}(x)\left[\frac{p^2}{2m} + V(x)\right]\Psi_{\alpha}(x), \tag{2}$$

where $p^2/2m$ is the kinetic energy of electrons with uniform effective mass m, and the operators $\Psi_{\alpha}^{\dagger}(x)$ and $\Psi_{\alpha}(x)$ are field operators that create and destroy a conduction electron with spin α at point x, respectively. The Hamiltonian (2) includes the potential structure $V(x)$ of the junction as shown in Fig. 1. The band structure of the junction is discontinuous and changes by the amount V_0 at the ferromagnet-insulator interfaces. In equilibrium the barrier is considered to be flat on top, while upon biasing the junction the potential of the barrier acquires a slope and the chemical potential μ^R in the right lead undergoes a shift eV with respect to the chemical potential μ^L in the left lead. Simultaneously, the conduction-band bottom V^R in the right lead shifts by eV with respect to the conduction-band bottom V^L in the left lead. The corresponding single-particle potential can then be written as

$$V(x) = \left[V_0 - eV\frac{x-\mathcal{L}}{\mathcal{R}-\mathcal{L}}\right]\Theta(x-\mathcal{L})\Theta(\mathcal{R}-x) - eV\Theta(x-\mathcal{R}). \tag{3}$$

The dispersion law for conduction electrons is taken in the effective-mass approximation as $\epsilon^{L(R)} = \hbar^2 q_{L(R)}^2/2m$ for the left and right lead, respectively, where $q_{L(R)} = \sqrt{2m(\hbar\omega - V^{L(R)})}/\hbar$ and m is the effective mass.

Expressing the localized character of the exchange interaction between s and d electrons by a delta function, we write the interacting part of the Hamiltonian as

$$H_{s\text{-}d} = -\frac{J}{2}\sum_{p;\alpha,\beta} \boldsymbol{\sigma}_{\alpha\beta}\cdot\mathbf{S}_p \int dx\, \Psi_{\alpha}^{\dagger}(x)\,\delta(x-x_p)\Psi_{\beta}(x), \tag{4}$$

where J is the coupling constant with units $\mathrm{J\,m}^d$ and d the dimension of the system. In Eq. (4) it is summed over all spins $\mathbf{S}_p$ in the system; $\boldsymbol{\sigma}_{\alpha\beta}$ is the vector of Pauli matrices, used to represent the spin of the conduction electrons that couple to the local moments $\mathbf{S}_p$. The indices α and β label the two spin projections: $\alpha,\beta \in \{\uparrow,\downarrow\}$. To obtain the effective indirect interaction between uncompensated magnetic moments of d electrons, we average $H_{s\text{-}d}$ in the subspace of conduction electrons and replace the conduction electron operators by a c number,

$$H_{\mathrm{eff}} = -\frac{J}{2}\sum_{p;\alpha,\beta} \boldsymbol{\sigma}_{\alpha\beta}\cdot\mathbf{S}_p\langle\Psi_{\alpha}^{\dagger}(x_p)\Psi_{\beta}(x_p)\rangle. \tag{5}$$

Since we are only interested in the relative orientation of the magnetized ferromagnets that are well below their critical point, we introduce a further approximation and substitute $\boldsymbol{\sigma}_{\alpha\beta}\cdot\mathbf{S}_p$ in H_{eff} by $\sigma_{\alpha}\langle S_p^z\rangle$ so that

$$H_{\mathrm{eff}} = -\frac{J}{2}\sum_{p} \langle S_p^z\rangle\Delta\rho(x_p), \tag{6}$$

where $\Delta\rho(x_p) = \Sigma_{\alpha}\sigma_{\alpha}\langle\Psi_{\alpha}^{\dagger}(x_p)\Psi_{\beta}(x_p)\rangle$ is the net spin polarization of the conduction electrons. In the following, we derive two approximations of the model: the mean-field approximation and the perturbation expansion.

A. Mean-field model

The mean-field approximation of the exchange interaction in Eq. (5) allows comparison to the theories by Julliere[4] and Slonzewski.[13] The magnetization of the d-electron system removes the spin degeneracy in the system of conduction electrons and this leads to a shift in the energy levels for the different spin projections similar to that induced by an external field in the Pauli theory of paramagnetism. If we consider semi-infinite ferromagnets, we can include the mean-field contribution to the magnetization of conduction electrons in an isotropic dispersion law for the two leads,

$$\epsilon_{\alpha}^{L(R)} = \epsilon^{L(R)} - \mu_0 h_{\alpha}^{L(R)}, \tag{7}$$

where $h_{\alpha}^{L(R)} = \sigma_{\alpha} h_0^{L(R)}$. The internal magnetic mean field in the respective lead is $h_0^{L(R)} = \langle S_{L(R)}^z\rangle J\rho^{L(R)}/2\mu_0$, where $\mu_0 = e\hbar/2m$ is the Bohr magneton, $\rho^{L(R)}$ the spin density, and $\langle S_{L(R)}^z\rangle$ depends on the spin orientation of each ferromagnet. To avoid ambiguities in the definitions, we assume that $\langle S_L^z\rangle$ is fixed to be positive, so that $\sigma_{\uparrow} = 1$ for majority spins and $\sigma_{\downarrow} = -1$ for minority spins in the left ferromagnet. Within the mean-field approximation the fluctuations arising in H_{eff} are omitted and thus the interacting part of the Hamiltonian is replaced by including relation (7) in the potential $V(x)$ in Eq. (2), so that H_0 turns into a two-band Hamiltonian

$$V_{\alpha}(x) = \mu_0 h_{\alpha}^{L}\Theta(\mathcal{L}-x) + \left[V_0 - eV\frac{x-\mathcal{L}}{\mathcal{R}-\mathcal{L}}\right] \times \Theta(x-\mathcal{L})\Theta(\mathcal{R}-x) + [\mu_0 h_{\alpha}^{R} - eV]\Theta(x-\mathcal{R}). \tag{8}$$

The mean-field model holds in cases of strong ferromagnetism but neglects finite-size effects here, arising from the

finite length of the ferromagnetic layers. This will be significant when we want to calculate the exchange interaction out of equilibrium.

B. Perturbation model

As opposed to calculations in the mean-field model where the ordering in the ferromagnets is incorporated *a priori* via the dispersion relation (7), calculations in the perturbation model first take into account the interaction between the individual pairs of spins in the different ferromagnets and includes their ordering within the ferromagnets afterwards by integrating over all spins of the individual ferromagnets. To obtain explicit expressions for the spin current and the interlayer exchange in this model, we expand perturbatively the average $\langle \Psi^{\dagger}_{\alpha}(x_p)\Psi_{\beta}(x_p)\rangle$ in Eq. (5). As long as the coupling constant J between s and d electrons is small compared to the Fermi energy in the respective lead, which is the case for a wide range of weak ferromagnetism, the perturbation model can certainly be regarded as valid.

The electronic band structure, described by $V(x)$ in Eq. (3) in the perturbation model or $V_{\alpha}(x)$ in Eq. (8) in the mean-field model, varies at the barrier on length scales that are short compared to the mean free path of the conduction electrons. Further, it is strongly influenced by the bias when measuring electronic properties of the structure so that the assumption that the system is close to equilibrium cannot be maintained in general. In order to establish a theoretical description of spin currents and interlayer exchange from first principles, we employ the Keldysh nonequilibrium perturbation formalism[41] along with a coupling procedure for structured systems developed by Caroli *et al.*[17–20] and Feuchtwang,[21–23] leading to a proper nonequilibrium field theoretic description. Since the treatments by Caroli and Feuchtwang are proper many-body formalisms, their application to the present problem would also provide the basis for the inclusion of further many-body effects such as carrier-carrier or carrier-magnon interactions to the problem.

III. RELATION BETWEEN SPIN-POLARIZED TUNNEL CURRENT AND INTERLAYER MAGNETIC-EXCHANGE COUPLING

Emphasizing the physical arguments, we outline in this section the relation between the spin-polarized tunnel current and the interlayer exchange coupling. Initially, we need to clarify what is meant exactly by interlayer exchange coupling and spin-polarized tunnel current. In our model the interlayer exchange coupling is the energy difference when two ferromagnetic slabs have parallel or antiparallel alignment with respect to each other. When the junction is biased out of equilibrium, a current of spin-polarized electrons tunnels through the barrier with characteristics that depend on the relative orientation of the ferromagnets. While interlayer exchange coupling occurs already in equilibrium, the spin-polarized tunnel current is a purely nonequilibrium effect. However, out of equilibrium the interlayer exchange coupling has terms related to the spin-polarized tunnel current that can dominate the coupling behavior under certain conditions.[38]

As pointed out before, the interaction between the localized moments of the different ferromagnets is mediated by spin-polarized conduction electrons. Thus, the exchange interaction is similar to the usual RKKY interaction where the interaction arises because a single spin impurity polarizes the conduction electrons around it, leading to a net spin polarization $\Delta\rho=\rho_{\uparrow}-\rho_{\downarrow}$. Because the system has a finite Fermi surface, the perturbation will oscillate with distance from the spin impurity with declining intensity similar to charge density oscillations of an electron gas. Accordingly, the orientation between slabs of spins varies between parallel and antiparallel alignment with a characteristic oscillation that depends on the Fermi wave vector and the distance between the slabs.

If a bias is applied across the junction, as is shown in Fig. 1, the electron spin polarization is altered by the nonequilibrium current of spin-polarized electrons. This contribution to the spin polarization is reflected in the difference between the current for spin-up and the current for spin-down conduction electrons that tunnel through the barrier,

$$\langle \mathcal{I}_{spt}\rangle=\langle \mathcal{I}_{\uparrow}\rangle-\langle \mathcal{I}_{\downarrow}\rangle. \tag{9}$$

It is therefore referred to as spin-polarized tunnel current, which arises from the perturbation of the conduction electrons by localized moments in each ferromagnet individually, and is proportional to a current of magnetization,

$$\langle \mathcal{I}_{M}\rangle=\frac{\mu_0}{e}\langle \mathcal{I}_{spt}\rangle. \tag{10}$$

We would like to point out that for a spin current to flow a single ferromagnet would be sufficient. On the other hand, as in the equilibrium case, each ferromagnet is perturbed by the spin current of the other ferromagnet thereby leading to an additional, spin-current-dependent contribution in the effective interaction between the two ferromagnets.

This connection between spin current and exchange interaction, whose detailed calculations we present in the following, is the origin of the unexpected effect, found by Schwabe *et al.*, that the presence of a nonequilibrium bias across a junction significantly alters the range of exchange interaction such that the interaction energy between two slabs of spins is proportional to their thickness.[38] In other words, the energy arising from this RKKY-like interaction between the different slabs does not converge to a finite limit for $l_{L(R)}\to\infty$ and therefore appears to act as an uniform magnetic field.

IV. NONEQUILIBRIUM FORMALISM

In order to calculate perpendicular transport and exchange interaction in a ferromagnet insulator ferromagnet from first principles, we have to apply proper nonequilibrium theories since for tunnel junctions the assumption that the system is close to equilibrium does generally not hold. By applying Keldysh's nonequilibrium perturbation formalism, Caroli *et al.*[17–20] and Feuchtwang[21–23] devised a theory that joins initially uncoupled subsystems through appropriate transfer terms to a single nonequilibrium steady-state system that only depends on the electron occupation numbers of the reservoirs.[42] Here we extend the formalism to include the electron spin. Furthermore, we rewrite the unperturbed Keldysh Green's functions $G^{</>}$ in terms of a superposition of spectral functions.

Keldysh's nonequilibrium perturbation theory is based on a time-loop integral with two separate branches: one *forward* in time and the other *backward* that replace the normal-time integral in regular perturbation theory. This has the advantage that the *S*-matrix expansion starts and ends with the same known state. The Green's functions within this formalism can be defined similarly to the usual ones, with the main difference that the concept of contour ordering replaces the usual time ordering. Depending on the relative positions of the time variables on the contour, four independent types of Green's functions are obtained,

$$G^{<}_{\alpha\beta}(x,t;x',t')=i\langle\Psi^{\dagger}_{\beta}(x',t')\Psi_{\alpha}(x,t)\rangle, \tag{11}$$

$$G^{>}_{\alpha\beta}(x,t;x',t')=-i\langle\Psi_{\alpha}(x,t)\Psi^{\dagger}_{\beta}(x',t')\rangle, \tag{12}$$

$$G^{r}_{\alpha\beta}(x,t;x',t')=-i\Theta(t)\langle\{\Psi^{\dagger}_{\beta}(x',t'),\Psi_{\alpha}(x,t)\}\rangle, \tag{13}$$

$$G^{a}_{\alpha\beta}(x,t;x',t')=i\Theta(-t)\langle\{\Psi^{\dagger}_{\beta}(x',t'),\Psi_{\alpha}(x,t)\}\rangle, \tag{14}$$

where the information of the system on its statistical properties is given by the Keldysh Green's functions $G^{</>}$ and on its dynamical behavior by the usual retarded and advanced Green's functions $G^{r/a}$. The curly braces in Eqs. (13) and (14) denote the anticommutator for fermions.

In steady state the time-loop *S*-matrix expansion translates into an operational rule for Keldysh operators,

$$(AB)^{</>}=A^{</>}B^{a}+A^{r}B^{</>}, \tag{15}$$

where the part with the retarded Green's function relates to the *forward* time branch and the part with the advanced Green's function to the *backward* one. Out of equilibrium the two branches give different results. Because of the steady-state character of our system, we Fourier transform in the following all Green's functions into the frequency domain.

To employ the nonequilibrium theories of Caroli *et al.* and Feuchtwang, it appears from Fig. 1 that a partitioning into three subsystems seems to be most appropriate: two ferromagnets, which form the leads that are connected to the reservoirs with the chemical potentials $\mu^{L(R)}$ and the intermediate region of the barrier. Accordingly, the Hamiltonian H_0 (2) is written as a sum of three independent parts,

$$H_0(x)=\Theta(\mathcal{L}-x)H_L(x)+\Theta(x-\mathcal{L})\Theta(\mathcal{R}-x)H_I(x)+\Theta(x-\mathcal{R})H_R(x), \tag{16}$$

to yield the following inhomogeneous Schrödinger equation:

$$[\omega-H_0(x)]G_{\alpha}(x,x';\omega)=\delta(x-x') \tag{17}$$

for the full system whereas the inhomogeneous Schrödinger equation for the subsystem can be written as

$$[\omega-H_p(x)]g_{p,\alpha}(x,x';\omega)=\delta(x-x'), \tag{18}$$

for the several uncoupled subparts of the system $p\in\{L,I,R\}$, where x, x' lie within the appropriate region determined by the choice of p. To keep our notation consistent, we do not drop the spin index for the uncoupled Green's function of the intermediate region, although in our model $g_{I,\uparrow}=g_{I,\downarrow}$.

To join the subsystems, we use the Feuchtwang approach since it has the advantage that properties of the continuous coupled system can be obtained in a mathematically straightforward manner by using Green's theorem. This method is analogous to solving the problem of diffraction of an electromagnetic wave on a dielectric material. According to Green's theorem, the Green's functions in Eqs. (17) and (18) have to satisfy appropriate boundary conditions at the electrode-barrier interfaces $\mathcal{R}$ and $\mathcal{L}$. The requirement for these Green's functions to fulfill boundary conditions is similar to the requirement to match wave functions in media with interfaces. For simplicity, we choose Dirichlet conditions so that the Green's functions vanish if they are taken with one of their arguments on the respective interfaces $\mathcal{R}$ or $\mathcal{L}$. In the particular case of our quasi-one-dimensional system these lead to simple algebraic equations. The unperturbed two-band Green's functions G_{α} read as

$$G_{\alpha}(x\in L,x')=\theta(\mathcal{L}-x')g_{L,\alpha}(x,x')+\chi_{L,\alpha}(x,\mathcal{L})G_{\alpha}(\mathcal{L},x'), \tag{19}$$

$$G_{\alpha}(x,x'\in L)=\theta(\mathcal{L}-x)g_{L,\alpha}(x,x')+G_{\alpha}(x,\mathcal{L})\chi_{L,\alpha}(\mathcal{L},x'), \tag{20}$$

$$G_{\alpha}(x\in R,x')=\theta(x'-\mathcal{R})g_{R,\alpha}(x,x')-\chi_{R,\alpha}(x,\mathcal{R})G_{\alpha}(\mathcal{R},x'), \tag{21}$$

$$G_{\alpha}(x,x'\in R)=\theta(x-\mathcal{R})g_{R,\alpha}(x,x')-G_{\alpha}(x,\mathcal{R})\chi_{R,\alpha}(\mathcal{R},x'), \tag{22}$$

where the frequency argument has been omitted, x,x' are defined in the full system, if not stated otherwise, and

$$\chi_{p,\alpha}(\mathcal{P},x')=\frac{\hbar^2}{2m}\partial_{x_1}g_{p,\alpha}(x_1,x')\big|_{x_1=\mathcal{P}},$$

$$\chi_{p,\alpha}(x,\mathcal{P})=\frac{\hbar^2}{2m}\partial_{x_1}g_{p,\alpha}(x,x_1)\big|_{x_1=\mathcal{P}}, \tag{23}$$

where $p\in\{L,R\}$, $\mathcal{P}\in\{\mathcal{L},\mathcal{R}\}$, and the appropriate spatial limit is taken in approaching $\mathcal{L}$ and $\mathcal{R}$ for functions defined in the respective subregions. In simple cases where $x,x'\in\{\mathcal{L},R\}$, the full Green's function can be written as

$$\begin{pmatrix} G_{\alpha}(\mathcal{L},\mathcal{L}) & G_{\alpha}(\mathcal{L},\mathcal{R}) \\ G_{\alpha}(\mathcal{R},\mathcal{L}) & G_{\alpha}(\mathcal{R},\mathcal{R}) \end{pmatrix} = \frac{2m}{\hbar^2}\frac{1}{D_{\alpha}}\begin{pmatrix} \gamma_{R,\alpha}(\mathcal{R},\mathcal{R})+\gamma_{I,\alpha}(\mathcal{R},\mathcal{R}) & \gamma_{I,\alpha}(\mathcal{L},\mathcal{R}) \\ \gamma_{I,\alpha}(\mathcal{R},\mathcal{L}) & \gamma_{L,\alpha}(\mathcal{L},\mathcal{L})+\gamma_{I,\alpha}(\mathcal{L},\mathcal{L}) \end{pmatrix}, \tag{24}$$

where

$$D_{\alpha}=[\gamma_{R,\alpha}(\mathcal{R},\mathcal{R})+\gamma_{I,\alpha}(\mathcal{R},\mathcal{R})][\gamma_{L,\alpha}(\mathcal{L},\mathcal{L})+\gamma_{I,\alpha}(\mathcal{L},\mathcal{L})]-\gamma_{I,\alpha}(\mathcal{L},\mathcal{R})\gamma_{I,\alpha}(\mathcal{R},\mathcal{L}) \tag{25}$$

and

$$\gamma_{p,\alpha}(\mathcal{P},\mathcal{Q}) = -\frac{\hbar^2}{2m}\partial_x\partial_{x'}g_{p,\alpha}(x,x';\omega)\big|_{x=\mathcal{P},x'=\mathcal{Q}}, \quad (26)$$

where $p\in\{L,I,R\}, \mathcal{P},\mathcal{Q}\in\{\mathcal{L},\mathcal{R}\}$. Analytical continuation $\omega \rightarrow \lim_{\delta\rightarrow 0^+}(\omega \pm i\delta)$ transforms the above Green's functions into retarded or advanced versions. The coupling procedure has enabled us to express the infinite open system in terms of the three subsystems where the information of the leads is contained in $\gamma_{L(R),\alpha}$. The denominator D_α contains the terms proportional to a self-energy that arises from the coupling of the system to reservoirs.

The Keldysh Green's functions $G^{</>}$ describe the statistical properties of the system. Since the decoupled regions are in equilibrium, they have well-defined electron occupations n_F^p, $p\in\{L,I,R\}$, and therefore the Keldysh Green's function for the subparts $g_{p,\alpha}^{</>}$ can be expressed as

$$g_{p,\alpha}^{<}(x,x') = n_F^p[g_{p,\alpha}^{a}(x,x') - g_{p,\alpha}^{r}(x,x')], \quad (27)$$

$$g_{p,\alpha}^{>}(x,x') = [n_F^p - 1][g_{p,\alpha}^{a}(x,x') - g_{p,\alpha}^{r}(x,x')]. \quad (28)$$

According to Ref. 42, the system ceases to depend on the occupation number of the intermediate region so that the unperturbed Green's function $G_\alpha^<$ is given as a superposition of terms that depend only on the properties of one or other grand canonical ensemble for the reservoirs where the respective electron occupations $n_F^{L(R)}$ are associated with corresponding spectral functions defined by $A_{L(R),\alpha}$. We can therefore write the Green's function $G_\alpha^<$ with help of the space representation of the spectral functions as

$$G_\alpha^<(x,x') = n_F^L A_{L,\alpha}(x,x') + n_F^R A_{R,\alpha}(x,x'). \quad (29)$$

The spectral functions $A_{L(R),\alpha}$ tell us about the nature of allowed electron states regardless of whether these states are occupied or not; on the other hand, the Green's function $G_\alpha^<$ tells us how many of these states are occupied. In the case where the arguments x,x' are at the interfaces $\mathcal{P},\mathcal{Q}\in\{\mathcal{L},\mathcal{R}\}$,

$$A_{L,\alpha}(\mathcal{P},\mathcal{Q}) = i\hbar v_{L,\alpha} G_\alpha^r(\mathcal{P},\mathcal{L}) G_\alpha^a(\mathcal{L},\mathcal{Q}), \quad (30)$$

$$A_{R,\alpha}(\mathcal{P},\mathcal{Q}) = i\hbar v_{R,\alpha} G_\alpha^r(\mathcal{P},\mathcal{R}) G_\alpha^a(\mathcal{R},\mathcal{Q}), \quad (31)$$

where

$$v_{L(R),\alpha} = -\frac{i\hbar}{2m}(\tilde{\gamma}_{L(R),\alpha}^a - \tilde{\gamma}_{L(R),\alpha}^r), \quad (32)$$

are the electron velocities and $\tilde{\gamma}_{L(R),\alpha}^r = \gamma_{L(R),\alpha}^r[\mathcal{L}(\mathcal{R}),\mathcal{L}(\mathcal{R})]$. A similar case holds for $G_\alpha^>$, which describes how many states of the system are empty. To obtain the corresponding expressions for $G_\alpha^>$, $n_F^{L(R)}$ has to be replaced by $n_F^{L(R)}-1$ according to Eq. (28).

V. SPIN-POLARIZED TUNNEL CURRENT

The formulations by Landauer and Büttiker for currents through a finite region of noninteracting electrons have contributed significantly to the clear understanding of mesoscopic transport as long as it is coherent across the device. If one uses phenomenological approaches to calculate the transmission functions, the Landauer-Büttiker formalism is particularly simple, and Bauer uses this method to calculate the perpendicular transport in metallic magnetic multilayers.[43] The quantum version of the Landauer formalism was used by Barnaś and Fert to describe coherent transport across a single interface between a ferromagnet and a nonmagnetic metal.[44] In this section, we will show that our results for the spin current can also be understood within the framework of the Landauer-Büttiker formalism. In order to derive the spin current, we first calculate the ensemble-averaged spin-dependent current operator in second quantization by means of Keldysh's nonequilibrium perturbation theory.

The spin-dependent current operator for the conduction electrons in second quantization reads as

$$\mathcal{I}_{\alpha\beta} = \frac{ie\hbar}{2m}[(\nabla\Psi_\beta^\dagger)\Psi_\alpha - \Psi_\beta^\dagger(\nabla\Psi_\alpha)], \quad (33)$$

so that we obtain for the ensemble-averaged spin-dependent current

$$\langle\mathcal{I}_{\alpha\beta}\rangle = \lim_{\mathbf{r}',t'\rightarrow\mathbf{r},t}\left[\frac{ie\hbar}{2m}(\nabla_{\mathbf{r}'} - \nabla_{\mathbf{r}})\right]\langle\Psi_\beta^\dagger(\mathbf{r}',t')\Psi_\alpha(\mathbf{r},t)\rangle. \quad (34)$$

The average $\langle\Psi_\beta^\dagger(\mathbf{r}',t')\Psi_\alpha(\mathbf{r},t)\rangle$ can be written in terms of the Keldysh Green's function (11). Due to the stationary state character of the present problem the continuity equation $\nabla\langle\mathcal{I}_{\alpha\beta}\rangle = 0$ holds, which allows us to calculate the current at an arbitrary point in the system. For one-dimensional cases, it is possible to write Eq. (34) as

$$\langle\mathcal{I}_{\alpha\beta}\rangle = \frac{e\hbar^2}{2m}\int_{-\infty}^{\infty}\frac{d\omega}{2\pi}\lim_{x'\rightarrow x}(\partial_{x'} - \partial_x)G_{\alpha\beta}^<(x,x';\omega), \quad (35)$$

where we took the Fourier transform into the frequency domain and expressed the average $\langle\Psi_\beta^\dagger(x')\Psi_\alpha(x)\rangle$ by the Keldysh Green's function $G^<$. Because our system is quasi-one-dimensional, the extensions to higher dimensions are achieved by means of Fourier transforms of the coordinates parallel to the barrier so that

$$G_\alpha(x,x';\mathbf{k}_\parallel;\omega) = \int_{-\infty}^{\infty} d^2x\, e^{i\mathbf{k}_\parallel\cdot\mathbf{x}} G_\alpha(\mathbf{r},\mathbf{r}';\omega), \quad (36)$$

where $\mathbf{r}$ is the three-dimensional coordinate, $\mathbf{x} = \mathbf{r}_\parallel - \mathbf{r}_\parallel'$ is the two-dimensional relative position vector parallel to the barrier, and $\mathbf{k}_\parallel$ denotes the two-dimensional electron wave vector parallel to the barrier. Similarly, Eq. (34) becomes

$$\langle\mathcal{I}_{\alpha\beta}^{3D}\rangle = \frac{e\hbar^2\rho^{3D}}{2m}\int_{-\infty}^{\infty}\frac{d^2k_\parallel}{(2\pi)^2}\int_{-\infty}^{\infty}\frac{d\omega}{2\pi}\lim_{x'\rightarrow x}(\partial_{x'} - \partial_x) \times G_{\alpha\beta}^{<3D}(x,x';\mathbf{k}_\parallel;\omega), \quad (37)$$

where the spins in the ferromagnet are assumed to be distributed uniformly and to have the same spin orientation such that ρ^{3D} represents the density of localized spins.

The extension to three dimensions leaves the spatial dependence of the Hamiltonian unaffected in the direction perpendicular to the barrier and only leads to a change in the

frequency arguments of the corresponding Green's functions (cf. Sec. IV). Therefore, we focus initially on the one-dimensional case and extend this to full three-dimensional version only at the end. Furthermore, since spin-flip processes are neglected throughout, the tensor $\langle \mathcal{I}_{\alpha\alpha}\rangle = \langle \mathcal{I}_\alpha\rangle$ is diagonal. In the following, by applying the nonequilibrium coupling theory of Feuchtwang, we reexpress the spin current in terms of local quantities to obtain Landauer-type formulas for the mean-field and perturbation model.

A. Spin-polarized tunnel current in mean-field model

In the mean-field model the full Green's function in Eq. (35) is replaced by the single-particle Green's function of the Hamiltonian (2) with the spin-dependent potential $V_\alpha(x)$ (8) and inserted into Eq. (9),

$$\langle \mathcal{I}_{spt}^{\mathrm{MF}}\rangle = \frac{e\hbar^2}{2m}\sum_\alpha \sigma_\alpha \int_{-\infty}^{\infty}\frac{d\omega}{2\pi}\lim_{x'\to x}(\partial_{x'}-\partial_x)G_\alpha^<(x,x'), \tag{38}$$

where the frequency argument is dropped for convenience from now on and the superscript (MF) denotes that the spin current is calculated within the mean-field approximation. Here, the nonequilibrium bias of the system is contained implicitly in the expression for $G_\alpha^<$. We need to incorporate the properties of the system, such as information about the barrier and leads coupled to different reservoirs, directly into the calculation.

Using $G_\alpha^a - G_\alpha^r = G_\alpha^< - G_\alpha^>$ [cf. Eqs. (29) and (B1)], differentiating, and taking the limit at the partition $\mathcal{L}$, for example, we transform the spin current (35) into

$$\langle \mathcal{I}_{spt}^{\mathrm{MF}}\rangle = \frac{e\hbar^2}{2m}\sum_\alpha \sigma_\alpha \int_{-\infty}^{\infty}\frac{d\omega}{2\pi}[G_\alpha^<(\mathcal{L},\mathcal{L})\tilde{\gamma}_{L,\alpha}^> - G_\alpha^>(\mathcal{L},\mathcal{L})\tilde{\gamma}_{L,\alpha}^<]. \tag{39}$$

Inserting the expressions for $G_\alpha^{</>}(\mathcal{L},\mathcal{L})$ into Eq. (39), and replacing $\tilde{\gamma}_{L,\alpha}^<$ and $\tilde{\gamma}_{L,\alpha}^>$ with the corresponding expressions in terms of their retarded and advanced Green's function by using the differentiated versions of Eqs. (27) and (28), we obtain

$$\langle \mathcal{I}_{spt}^{\mathrm{MF}}\rangle = -e\hbar^2\sum_\alpha \sigma_\alpha \int_{-\infty}^{\infty}\frac{d\omega}{2\pi}(n_F^L - n_F^R) \times G_\alpha^a(\mathcal{L},\mathcal{R})G_\alpha^r(\mathcal{R},\mathcal{L})v_{L,\alpha}v_{R,\alpha}, \tag{40}$$

where $n_F^{L(R)} = \{\exp[\beta(\hbar\omega - \mu^{L(R)})]+1\}^{-1}$ are the occupation numbers of the reservoirs with chemical potentials $\mu^{L(R)}$. Although the spin-up and spin-down electrons are not coupled in this model, it is possible to assume that $\mu^{L(R)}$ are independent of spin and are set by the reservoirs that are implied to be in direct contact with the semi-infinite ferromagnetic slabs.[42] Since in the mean-field model fluctuations of individual spins are neglected so that their only contribution is a macroscopic change of the band structure, the nonequilibrium result (40) is analogous to a linear response expression derived previously by Tsymbal and Pettifor based on the Kubo-Greenwood formula.[39]

The term $\hbar^2 G_\alpha^a(\mathcal{L},\mathcal{R})G_\alpha^r(\mathcal{R},\mathcal{L})v_{L,\alpha}v_{R,\alpha}$ corresponds to the spin-dependent transmission coefficient through the intermediate region $T_\alpha(\omega)$ derived in Appendix A and with this identification takes the form of

$$\langle \mathcal{I}_{spt}^{\mathrm{MF}}\rangle = -e\sum_\alpha \sigma_\alpha \int_{-\infty}^{\infty}\frac{d\omega}{2\pi}(n_F^L - n_F^R)T_\alpha. \tag{41}$$

From this we see that calculating the spin current in the infinite open system is reduced to obtaining the spin-dependent transmission coefficient $T_\alpha(\omega)$. The statistical properties of the system are solely reflected in the difference of occupation numbers of the reservoirs represented by grand-canonical ensembles. The number of current-carrying states is different in the reservoirs to that in the structure and this requires a redistribution of the spin current among the states at the interface and thus leads to a spin-dependent interface resistance.

As pointed out before, the three-dimensional case does not introduce any new complications, so that the current at zero temperature is given as

$$\langle \mathcal{I}_{spt}^{\mathrm{3D,\,MF}}\rangle = -\frac{e}{\hbar}\frac{m\nu^{\mathrm{2D}}}{(2\pi\hbar)^2}\sum_\alpha \sigma_\alpha\left[\int_{-\mu_0 h_\alpha^L}^{\mu} d\epsilon(\mu-\epsilon) - \int_{-\mu_0 h_\alpha^R - eV}^{\mu - eV} d\epsilon(\mu - eV - \epsilon)\right]T_\alpha, \tag{42}$$

where $\mu = \mu_L$ and ν^{2D} is the surface area of the junction. The magnetic mean field of the ferromagnets now includes the three-dimensional spin density instead, so that $h_0^{L(R)} = \langle S_{L(R)}^z\rangle J\rho_{L(R)}^{\mathrm{3D}}/(2\mu_0)$.

B. Spin-polarized tunnel current in perturbation model

Turning to the perturbation model and thus neglecting the spin splitting of the bands in the dispersion relation (7), the transmission coefficients will be the same for different spin orientations and consequently Eq. (41) vanishes. However, we examine what happens if we include the expansion of the interacting part of the Hamiltonian H_{eff} instead. Thus, we have to expand $G_{\alpha\beta}^{</>}$ of the full interacting system in terms of the Green's function $G^{</>}$ of the unperturbed single-band Hamiltonian H_0. Using Eq. (15), we calculate the Green's function $G^{</>}$ to first order in H_{eff} (5),

$$G_{(1)\alpha\beta}^{</>}(x,x';\omega) = G^{</>}(x,x';\omega)\delta_{\alpha\beta} - \frac{J}{2}\sum_p \langle \mathbf{S}_p\cdot\boldsymbol{\sigma}_{\beta\alpha}\rangle \times [G^{</>}(x,x_p;\omega)G^a(x_p,x';\omega) + G^r(x,x_p;\omega)G^{</>}(x_p,x';\omega)]. \tag{43}$$

Dropping the frequency argument and neglecting spin fluctuations, this gives the first-order perturbation expression of the spin current $\langle \mathcal{I}_{spt}\rangle$ in Eq. (9),

$$\langle \mathcal{I}_{spt}^{\mathrm{Per}}\rangle = -\frac{e\hbar^2 J}{2m}\sum_p \langle S_p^z\rangle \int_{-\infty}^{\infty}\frac{d\omega}{2\pi}C^{\mathrm{Per}}(x_p), \tag{44}$$

where the superscript (Per) denotes the perturbation treatment of the problem and

$$C^{\mathrm{Per}}(x_p)=\lim_{x'\to x}(\partial_{x'}-\partial_x)[G^<(x,x_p)G^a(x_p,x') + G^r(x,x_p)G^<(x_p,x')]. \tag{45}$$

In the present case of a continuous system, we replace the sum over all spins on either side of the barrier in Eq. (44) by a spatial integration,

$$\langle\mathcal{I}^{\mathrm{Per}}_{spt}\rangle=\langle\mathcal{I}^{\mathrm{Per}}_{spt,L}\rangle+\langle\mathcal{I}^{\mathrm{Per}}_{spt,R}\rangle, \tag{46}$$

where

$$\langle\mathcal{I}^{\mathrm{Per}}_{spt,L(R)}\rangle=-\frac{e\hbar^2 J\rho^{L(R)}}{2m}\langle S^z_{L(R)}\rangle\int_{\mathcal{L}-l_L}^{\mathcal{L}}\left(\int_{\mathcal{R}}^{\mathcal{R}+l_R}\right)dx_{L(R)} \times\int_{-\infty}^{\infty}\frac{d\omega}{2\pi}C^{\mathrm{Per}}(x_{L(R)}); \tag{47}$$

as before $\langle S^z_{L(R)}\rangle$ depends on the spin orientation of each ferromagnet, and $\rho^{L(R)}$ is its density of localized spins. A position within the left ferromagnet is indicated by x_L and within the right one by x_R, respectively. The contribution $\langle\mathcal{I}^{\mathrm{Per}}_{spt}\rangle$ to the spin current depends on two terms: one originating from the left ferromagnet and another from the right ferromagnet.

Again reexpressing the Green's functions G in terms of their local expressions, the basic principles used for $\langle\mathcal{I}^{\mathrm{MF}}_{spt}\rangle$ are repeated for the evaluation of $\langle\mathcal{I}^{\mathrm{Per}}_{spt}\rangle$. Inserting Eqs. (19)–(22) into Eq. (45), using $G^a_\alpha-G^r_\alpha=G^<_\alpha-G^>_\alpha$ as above, differentiating and taking the limit at the partition $\mathcal{L}$ or $\mathcal{R}$, we can write the integrand of the spin current (45) in the following form, depending on the location of the spin on either the left or right side of the system L,R,

$$C^{\mathrm{Per}}(x_p)=\frac{2m}{\hbar^2}[\tilde\chi^<_pG^>(\mathcal{P},\mathcal{P})-\tilde\chi^>_pG^<(\mathcal{P},\mathcal{P})] -[\tilde\gamma^<_pG^>(\mathcal{P},\mathcal{P})-\tilde\gamma^>_pG^<(\mathcal{P},\mathcal{P})][\tilde\chi^a_pG^a(\mathcal{P},\mathcal{P}) +\tilde\chi^r_pG^r(\mathcal{P},\mathcal{P})], \tag{48}$$

where $\tilde\chi_p=\chi_p(x_p,\mathcal{P})\chi_p(\mathcal{P},x_p)$, with $p\in\{L,R\}$, $\mathcal{P}\in\{\mathcal{L},\mathcal{R}\}$. Writing $G^{</>}$ with help of Eq. (29) and $\tilde\chi^{</>},\tilde\gamma^{</>}$ by differentiating Eqs. (27) and (28), we transform $C^{\mathrm{Per}}(x_p)$ into

$$C^{\mathrm{Per}}(x_p)=-\frac{2m}{\hbar^2}(n^L_F-n^R_F)T\left\{\left[G^a(\mathcal{P},\mathcal{P})-\frac{i}{\hbar v_p}\right]\tilde\chi^a_p+\mathrm{c.c.}\right\}, \tag{49}$$

where we replaced $\hbar^2G^a(\mathcal{L},\mathcal{R})G^r(\mathcal{R},\mathcal{L})v_Lv_R$ by the transmission coefficient $T(\omega)$ through the intermediate region (A5). In Eq. (49) the quantity $i/(\hbar v_p)$ is the amplitude of the unperturbed single-particle Green's function, whereas $G^a(\mathcal{P},\mathcal{P})$ with $\mathcal{P}\in\{\mathcal{L},\mathcal{R}\}$ relates to the amplitude of the full Green's function at the interface. Next, we spatially integrate over the ferromagnets. Because $\tilde\chi_{L(R)}$ is the only term depending on the integration variable $x_{L(R)}$, we define (cf. Appendix C)

$$\tilde\xi^{r/a}_{L(R)}=\frac{2mv_{L(R)}}{\hbar}\int_{\mathcal{L}-l_L}^{\mathcal{L}}\left(\int_{\mathcal{R}}^{\mathcal{R}+l_R}\right)dx_{L(R)}\tilde\chi^{r/a}_{L(R)}, \tag{50}$$

which is oscillatory and varies with the thickness of the ferromagnet. Finally, we can express the contributions to the spin current $\langle\mathcal{I}^{\mathrm{Per}}_{spt,\,p}\rangle, p\in\{L,R\}$, in terms of local quantities only:

$$\langle\mathcal{I}^{\mathrm{Per}}_{spt,p}\rangle=-2e\int_{-\infty}^{\infty}\frac{d\omega}{2\pi}(n^L_F-n^R_F)\,TN^p. \tag{51}$$

The difference between the usual Landauer formula and Eq. (51) lies in the dimensionless quantity

$$N^p=\frac{\mu_0h^p_0}{2\epsilon^p}\,\mathrm{Im}[r^r_{\mathcal{P}}\tilde\xi^r_p], \tag{52}$$

which reflects the amount of spin polarization from each ferromagnet. The first term in Eq. (52) $\mu_0h^p_0/\epsilon^p$ also arises in the theory of Pauli paramagnetism for one dimension. However, the magnetic field $h^p_0=\langle S^z_p\rangle J\rho^p/2\mu_0$ originates now from the spin order in the respective ferromagnet. The second term $\mathrm{Im}[r^r_{\mathcal{P}}\tilde\xi^r_p]$, where $r^r_{\mathcal{P}}=1-i\hbar v_pG^r(\mathcal{P},\mathcal{P})$ is a reflection amplitude (cf. Appendix A), arises due to spin-dependent reflection of conduction-electron waves at the respective barrier interface $\mathcal{P}\in\{\mathcal{L},\mathcal{R}\}$ back into the ferromagnet. It can vary only between -1 and 1 and becomes constant when the thickness of the ferromagnets is large since $\lim_{l_p\to\infty}(-i\tilde\xi^r_p)=1$. Thus, the oscillatory behavior of the spin polarization is due to the finite size of the ferromagnets and is similar to the fluctuations caused by an individual spin.

The spin polarization, which arises from the reflection off the barrier, is a quantum interference effect and can intuitively be understood from this calculation. In the model it is assumed that the Fermi energy in a particular lead is uniform upon biasing the junction so that the main effect of the bias is a net particle drift within that lead. We now probe the left ferromagnet with an electron incident from the left that interacts, depending on its spin orientation, with a localized spin so that it is either transmitted or reflected. If the electron is reflected its wave function interferes with the incoming unscattered wave of another electron in a way that depends on the reflection off the localized spin. From Eq. (33) it can be seen that a current is proportional to the difference in the probabilities of particle densities traveling in opposite directions. Because there are many spins in each ferromagnet, the oscillatory part $\tilde\xi_{L(R)}$ in Eq. (52) is a superposition of all waves from each individual scattering event and its amplitude depends on the reflection off the respective barrier interface. The contributions $\langle\mathcal{I}^{\mathrm{Per}}_{spt,p}\rangle$ to the spin current are proportional to the relative density of spin-polarized electrons reflected off of the respective side of the barrier, i.e., the difference between the densities for the reflected spin-up and spin-down conduction electrons. Consequently, the effect of the reflection off an interface leads to uniform spin polarization $N^p(\omega)$ or in other words to a spin-dependent interface resistance for the itinerant s electrons that interact with the localized d electrons. This leads to an interesting relation between the charge current and the spin current: whereas the charge current depends only on the transmission

coefficient $T(\omega)$, the spin current depends on the product of reflection amplitude $r^r_{\mathcal{P}}(\omega)$ and transmission coefficient $T(\omega)$.

Finally, for weak bias and low temperatures we assume that $T(\omega)$ is approximately constant so that we can transform Eq. (51) into

$$\langle \mathcal{I}^{\rm Per}_{spt,p}\rangle \approx -\frac{2e}{h}(\mu_L-\mu_R)\,T(\epsilon_F)\,\eta^p=\eta^p\langle \mathcal{I}_e\rangle, \qquad (53)$$

where $\langle \mathcal{I}_e\rangle$ is the usual Landauer expression for the charge current and

$$\eta^p=\frac{1}{eV}\int_{\mu-eV}^{\mu} d\epsilon\, N^p, \qquad (54)$$

the efficiency of polarizing conduction electron spins where we have set $\mu_L=\mu$ and $\mu_R=\mu-eV$, as before. Thus, $\eta^p(\epsilon_F)$ is equivalent to the phenomenological polarization constant that describes the efficiency of spin injection from ferromagnetic into superconducting metals in the experiments by Tedrow and Meservey[45] or from ferromagnetic into normal metals by Johnson and Silsbee.[15]

The three-dimensional case is treated similarly as before in the mean-field model so that the current is given at zero temperature as

$$\langle \mathcal{I}^{\rm 3D,\,Per}_{spt}\rangle=-\frac{2e}{\hbar}\frac{m\nu^{\rm 2D}}{(2\pi\hbar)^2}\Big[\int_0^{\mu} d\epsilon(\mu-\epsilon) - \int_{-eV}^{\mu-eV} d\epsilon(\mu-eV-\epsilon)\Big]T(N^L+N^R). \qquad (55)$$

VI. NONEQUILIBRIUM INTERLAYER MAGNETIC-EXCHANGE COUPLING

The interaction between the localized moments in ferromagnets is mediated by polarized conduction electrons. Schwabe *et al.* found that the presence of a nonequilibrium bias across a junction significantly alters the range of the RKKY-like interaction such that the interaction energy between two slabs of spins is proportional to their thickness.[38] Here, we relate this unexpected proportionality to the spin-polarized tunnel current of the perturbation model introduced in the previous section. Furthermore, we will point out that in the mean-field model there also exist terms in the coupling energy proportional to $\langle S^z_L\rangle\langle S^z_R\rangle$ that are equally related to a spin current.

The spin order in electronic systems is mainly due to the exchange interaction energy of electrons. For two ferromagnetic slabs this energy may be represented as

$$E_{\rm ex}=-A\langle S^z_L\rangle\langle S^z_R\rangle, \qquad (56)$$

where A is a parameter with units of energy which is a function that depends on the barrier properties and the size of the slabs, and $\langle S^z_p\rangle$ is the average spin polarization of the localized d electrons in the respective ferromagnet. If $A>0$ then the minimum of $E_{\rm ex}$ corresponds to parallel orientation of the slabs since $\langle S^z_L\rangle\langle S^z_R\rangle$ is positive; otherwise $A<0$ leads to an antiparallel alignment.

In $H_{\rm eff}$ as defined in Eq. (6) the localized spins in the two ferromagnets are treated separately. In the right ferromagnet the localized spins interact with the polarized conduction spin density arising from localized spins on the left side whereas in the left ferromagnet the localized spins interact with the polarized conduction spin density due to localized spins on the right side. The total exchange energy for spins on different sides of the barrier is thus the sum of these two contributions, from all n and m spins in the left and right ferromagnet, respectively.

$$E_{\rm ex}=-\frac{J}{2}\sum_{\substack{p=L_n,R_m\\ \alpha}}\sigma_\alpha\{\langle S^z_L\rangle\langle\Psi^\dagger_\alpha(x_p)\Psi_\beta(x_p)\rangle\}_{\rm ex}, \qquad (57)$$

where the sum is over all spin states and $\{\}_{\rm ex}$ denotes that only contributions between the ferromagnets but not within each of them are included. The spin-dependent particle density is expressed in terms of the Keldysh Green's function,

$$\langle\Psi^\dagger_\beta(x_p)\Psi_\alpha(x_p)\rangle=-i\hbar\int_{-\infty}^{\infty}\frac{d\omega}{2\pi}G^<_{\alpha\beta}(x_p,x_p;\omega). \qquad (58)$$

Again we discriminate between the mean field and the perturbation models.

A. Interlayer exchange in perturbation model

In the perturbation model considered in Ref. 38 the exact Green's function $G^<_{\alpha\beta}$ in Eq. (58) is replaced by its first-order approximation (43), so that $E_{\rm ex}$ in Eq. (57) gives

$$E^{\rm Per}_{\rm ex}=J^2\sum_{p=L_n,q=R_m}\langle S^z_p\rangle\langle S^z_q\rangle\,{\rm Im}\int_{-\infty}^{\infty}\frac{d\omega}{2\pi}G^<(x_p,x_q;\omega) \times[G^a(x_q,x_p;\omega)+G^r(x_q,x_p;\omega)]. \qquad (59)$$

For a single spin on each side of the barrier and equilibrium $E^{\rm Per}_{\rm ex}$ goes over into an expression that can be derived from a closed-loop Feynman diagram in conventional S-matrix theory,[46] such that

$$G^<(x_L,x_R)[G^a(x_R,x_L)+G^r(x_R,x_L)] =-2\,n_F\,{\rm Im}[G^r_\alpha(x_L,x_R)]^2.$$

This leads to a well-known expression for the RKKY interaction.[47] In other words, in equilibrium the Keldysh loop leads to the same results as conventional S-matrix theory as it should.

The expressions for the local Green's function, given in Sec. IV, replace the Green's functions G in Eq. (59), so that after carrying out similar manipulations to those for the spin current, and realizing that $G^a(\mathcal{P},\mathcal{Q})-G^r(\mathcal{P},\mathcal{Q})=A_R(\mathcal{P},\mathcal{Q})+A_L(\mathcal{P},\mathcal{Q})$ (see Appendix B), we obtain $E^{\rm Per}_{\rm ex}=E^{{\rm Per}(O)}_{\rm ex}+E^{{\rm Per}(I)}_{\rm ex}$, where

$$E^{{\rm Per}(O)}_{\rm ex}=\frac{\mu_0^2}{4\hbar}h_0^Lh_0^R\,{\rm Im}\int_{-\infty}^{\infty}\frac{d\omega}{2\pi}(n_F^L+n_F^R)(\hbar t^r)^2\frac{\tilde\xi^r_R}{\epsilon^r_R}\frac{\tilde\xi^r_L}{\epsilon^r_L}, \qquad (60)$$

$$E_{\rm ex}^{{\rm Per}(I)}=2\mu_0\int_{-\infty}^{\infty}\frac{d\omega}{2\pi}(n_F^L-n_F^R)T\left[h_0^L\frac{\xi_L^0}{v_L}N^R-h_0^R\frac{\xi_R^0}{v_R}N^L\right], \tag{61}$$

and

$$\xi_{L(R)}^0=\int_{\mathcal{L}-l_L}^{\mathcal{L}}\left(\int_{\mathcal{R}}^{\mathcal{R}+l_R}\right)dx_{L(R)}\,\chi_{L(R)}^r[x_{L(R)},\mathcal{L}(\mathcal{R})]\times\chi_{L(R)}^a[\mathcal{L}(\mathcal{R}),x_{L(R)}], \tag{62}$$

which varies for $\hbar\omega\geqslant V^{L(R)}$ as $l_{L(R)}$ with the thickness of the respective ferromagnet unlike $\tilde{\xi}_p^{r/a}$ in Eq. (50) and is exponentially damped for $\hbar\omega<0$ (cf. Appendix C). The dimensionless quantities N^p from Eq. (52) describe spin polarization from the ferromagnets and the transmission amplitude $t^r=-i\hbar\sqrt{v_Lv_R}\,G^r(\mathcal{L},\mathcal{R})$ is derived in Appendix A. The relation between transmission amplitude and transmission coefficient is given by $T(\omega)=|t^r(\omega)|^2$. For $\hbar\omega\geqslant V^p$, $E_{\rm ex}^{{\rm Per}(O)}$ is purely oscillatory in l_p, because in the case of our simplified model $\tilde{\xi}_p^r=-i[\exp(2iq_pl_p)-1]$. This contribution to the exchange energy is also present in the equilibrium case since in Eq. (60) $n_F^L+n_F^R=2n_F$. The second contribution to the exchange energy $E_{\rm ex}^{{\rm Per}(I)}$ is proportional to the length of the ferromagnets, since $\xi_p^0=l_p$, and thus is responsible for the unexpected behavior found in Ref. 38. Further, it vanishes in equilibrium, i.e., $n_F^L-n_F^R=0$, so that it represents the nonequilibrium polarization effect caused by the current of spin-polarized conduction electrons, as pointed out in Sec. III. In the remaining part of this section we want to discuss the term $E_{\rm ex}^{{\rm Per}(I)}$ in more detail. Before, we add the three-dimensional case of the interlayer exchange at zero temperature,

$$E_{\rm ex}^{{\rm 3D,\,Per}(O)}=\frac{m\nu^{\rm 2D}}{(2\pi\hbar)^2}\left[\int_0^{\mu}d\epsilon(\mu-\epsilon)+\int_{-eV}^{\mu-eV}d\epsilon(\mu-eV-\epsilon)\right]\times\left\{\frac{\mu_0^2h_0^Lh_0^R}{4}{\rm Im}\left[(t^r)^2\frac{\tilde{\xi}_R^r}{\epsilon_R^r}\frac{\tilde{\xi}_L^r}{\epsilon_L^r}\right]\right\}, \tag{63}$$

$$E_{\rm ex}^{{\rm 3D,\,Per}(I)}=\frac{m\nu^{\rm 2D}}{(2\pi\hbar)^2}\left[\int_0^{\mu}d\epsilon(\mu-\epsilon)-\int_{-eV}^{\mu-eV}d\epsilon(\mu-eV-\epsilon)\right]\times\left\{\frac{2\mu_0}{\hbar}T\left[h_0^L\frac{\xi_L^0}{v_L}N^R-h_0^R\frac{\xi_R^0}{v_R}N^L\right]\right\}, \tag{64}$$

where the magnetic mean field of the ferromagnets includes again the three-dimensional spin density.

In the quasi-one-dimensional system we are studying here, the important contributions to the exchange interaction are close to the Fermi surface of the respective lead, so that the electron velocities v_p can be replaced by their Fermi velocities v_p^F and Eq. (61) approximated by

$$E_{RK}^{{\rm Per}(I)}\approx\mu_0(h_{spt}^L\mathcal{N}^{l_R}\langle S_R^z\rangle-h_{spt}^R\mathcal{N}^{l_L}\langle S_L^z\rangle), \tag{65}$$

where the contributions from each ferromagnet to the spin-polarized tunnel current (51) define a magnetic field that is transported by spin-polarized conduction electrons,

$$h_{spt}^p=\frac{m}{e^2}\langle\mathcal{I}_{spt,p}^{\rm Per}\rangle. \tag{66}$$

Further, we have introduced new dimensionless quantities,

$$\mathcal{N}^{l_p}=\frac{J\rho_pl_p}{\hbar v_F^p}=\pi Jg(\epsilon_F^p)\,n_d^p, \tag{67}$$

where $n_d^p=\rho_pl_p$ gives the number of spins in the slabs and $g(\epsilon_F)=(\pi\hbar)^{-1}\sqrt{m/2\epsilon_F}$ is the one-dimensional density of states at the equilibrium Fermi energy of the respective lead. The dimensionless product $Jg=J/\pi\hbar v$, which is used to quantify the coupling constant J for the s-d interaction, can often be estimated from the Kondo temperature.[48] For the three-dimensional case we have to replace in Eq. (66) $\langle\mathcal{I}_{spt,p}^{\rm Per}\rangle$ by the expression (55), the number of localized spins n_d^p by $\tilde{n}_d^p=\rho_p^{\rm 3D}l_p\nu^{\rm 2D}$, and $g(\epsilon_F)$ by the quasi-one-dimensional density of states $\tilde{g}(\epsilon_F)=(\nu^{\rm 2D}\pi\hbar)^{-1}\sqrt{m/2\epsilon_F}$.

Since in a steady-state situation the spin current is independent of position, it carries information of local spin polarizations throughout the entire system and thus represents a nonlocal quantity. This property of the spin current should also be reflected in the exchange energy. Upon biasing the junction its symmetry is broken, so that a charge current is driven through the system, resulting in the occurrence of a ''current'' term $E_{\rm ex}^{{\rm Per}(I)}$ out of equilibrium. This term depends on the transmission coefficient, the spin polarization by the ferromagnets and the difference of the electron occupation in the reservoirs. We have shown in Eq. (66) that in correspondence to the different branches in the Keldysh loop, the exchange interaction in this term is related to a *forward* spin current from the left side of the barrier acting on spins on the right side and a *backward* spin current from the right side of the barrier acting on the spins on the left side. According to Eq. (10), this is the same as saying that $E_{\rm ex}^{{\rm Per}(I)}$ occurs via the interaction of the ferromagnet on the right side of the barrier with the nonequilibrium current of magnetization $\langle\mathcal{I}_M^L\rangle$ injected from the left ferromagnet and the interaction of the left ferromagnet with the nonequilibrium current of magnetization $\langle\mathcal{I}_M^R\rangle$ injected from the right ferromagnet. Thus, for the exchange interaction the field effect of the spin currents from different sides of the barrier subtracts rather than adds as occurs for the overall spin current in Eq. (46).

This fundamental difference is due to the fact that the exchange interaction depends on the induced spin densities while the spin current involves the difference in densities times velocities. Because the global direction of the charge current is defined from left to right, i.e., $\mu_L>\mu_R$, we find that the nonequilibrium effect on the interaction in $E_{\rm ex}^{{\rm Per}(b)}$ is proportional to $\langle\mathcal{I}_{spt,L}\rangle-\langle\mathcal{I}_{spt,R}\rangle$ if we assume identical ferromagnets and a constant Fermi velocity in Eq. (65). This result is different from that found for the spin current of the full system (46) that is $\langle\mathcal{I}_{spt,L}\rangle+\langle\mathcal{I}_{spt,R}\rangle$ for parallel alignment of the ferromagnets. It is only in the case of antiparallel alignment that the results are proportional. Later in Sec. VII

TABLE I. Parameters for the ferromagnet-barrier-ferromagnet tunnel junction described in the text. The ferromagnetic materials consist of either Ni or Fe and an insulator material of either Al_2O_3 or MgO. The exchange interaction between the d electrons within a single ferromagnet causes a splitting of their band bottoms into two different spin subbands that is proportional to $J\rho/\mu$.

Insulator	ϕ (eV)	s (Å)	Ferromagnet	μ (eV)	k_F (Å^{-1})	$J\rho/\mu$	l (Å)	V_0 (eV)	V_0/μ
MgO	0.9	21	Fe	5.0	1.26	0.32	80–250	5.9	1.18
Al_2O_3	1.8–3.5	12–18	Ni	5.0	1.26	0.58	80–250	6.8–8.5	1.36–1.7

we will present numerical examples to demonstrate this connection between spin current and exchange coupling.

Thus, we can now give the following explanation of the ferromagnetic slab size dependence in the exchange interaction found in Ref. 38. Upon biasing the system out of equilibrium, a steady-state current is driven across the junction so that in the ferromagnetic slabs conduction electrons interact with localized moments and become spin polarized. This creates an uniform magnetic field h^p_{spt} (66) carried by the spin-polarized current (51). Because the spin current is uniform throughout the system, the uniform magnetic field acts on the localized spins in the ferromagnet of the other side of the barrier. A uniform magnetic field acting on a spin system is proportional to the number of spins involved and thus the exchange interaction is also.

B. Interlayer exchange in mean-field model

In the mean-field model, $E_{\rm ex}$ in Eq. (57) derives from the interaction between localized spins and conduction electrons in different spin subbands, so that the unperturbed Green's function G_α differs for ferromagnetic and antiferromagnetic interlayer coupling. The nonlocal terms describing the exchange coupling across the barrier are already contained implicitly within the unperturbed Green's function G_α that replaces the exact Green's function $G^<_{\alpha\beta}$ in Eq. (58), leading to

$$E^{\rm MF}_{\rm ex}=-\frac{J}{2}\sum_{\substack{p=L_n,R_m\\ \alpha}}\sigma_\alpha\left\{\langle S^z_p\rangle\,{\rm Im}\int_{-\infty}^{\infty}\frac{d\omega}{2\pi}G^<_\alpha(x_p,x_p;\omega)\right\}_{\rm ex}. \tag{68}$$

The sum in Eq. (68) is over an infinite number of spins since we assumed semi-infinite slabs in the mean-field model. In this case, the resulting total spin moments per unit area are not strictly defined and we therefore assume that $l_{L(R)}$ is finite but large such that the mean-field approximation still holds well.

Replacing the sum over all spins in both ferromagnets by a spatial integration as in Eq. (50), we rewrite Eq. (68) entirely in terms of local functions as was done similarly in the previous cases, $E^{\rm MF}_{\rm ex}=E^{{\rm MF}(O)}_{\rm ex}+E^{{\rm MF}(I)}_{\rm ex}$, where

$$E^{{\rm MF}(O)}_{\rm ex}=\mu_0\sum_{\substack{p=L,R\\ \alpha}}\left\{h^p_\alpha\int_{-\infty}^{\infty}\frac{d\omega}{2\pi}n^p_F\,{\rm Im}\left[\frac{\hbar}{2\epsilon^r_{p,\alpha}}(1-r^r_{\mathcal{P},\alpha})\right]\right\}_{\rm ex} \tag{69}$$

$$E^{{\rm MF}(I)}_{\rm ex}=\mu_0\sum_\alpha\int_{-\infty}^{\infty}\frac{d\omega}{2\pi}(n^L_F-n^R_F)\times\left\{T_\alpha\left[h^L_\alpha\frac{\xi^0_{L,\alpha}}{v_{L,\alpha}}-h^R_\alpha\frac{\xi^0_{R,\alpha}}{v_{R,\alpha}}\right]\right\}_{\rm ex}, \tag{70}$$

and for consistency the limit for large ferromagnets was taken such that $-i\tilde{\xi}^r_{p,\alpha}=1$ in $E^{{\rm MF}(O)}_{\rm ex}$. Now the electron velocity, transmission coefficient, mean magnetic field, and reflection amplitude $r^r_{\mathcal{P},\alpha}=1-i\hbar v_{p,\alpha}G^r_\alpha(\mathcal{P},\mathcal{P})$, which arise from a wave being scattered off the respective barrier, are all spin dependent.

Because the exchange energy depends on the relative spin orientation of the two ferromagnets, we furthermore want to show that $E^{{\rm MF}(I)}_{\rm ex}$ has terms in $\langle S^z_L\rangle\langle S^z_R\rangle$. For this we assume a small band splitting relative to the Fermi energy in each ferromagnet, so that $v_{p,\alpha}\approx v_p(1-\mu_0h^p_\alpha/2\epsilon_p)$, and a thick barrier, such that its main contribution is an exponential damping. The spin current in the mean-field model (41) is thus approximated by

$$\langle\mathcal{I}^{\rm MF}_{spt,p}\rangle\approx-2e\int_{-\infty}^{\infty}\frac{d\omega}{2\pi}(n^L_F-n^R_F)\,T\frac{\mu_0h^p_0}{2\,\epsilon_p}. \tag{71}$$

This form of the spin current is rather intuitive since it is expressed as the probability of spin-polarized electrons tunneling through the barrier. The properties of the barrier are contained in the transmission coefficient T whereas the amount of spin polarization is determined by the Pauli factor $\mu_0h^p_0/2\,\epsilon_p$. Inserting Eq. (71) into Eq. (66), we obtain Eq. (65) for the nonequilibrium contribution $E^{{\rm MF}(I)}_{\rm ex}$ in analogy to the perturbation result. All terms in Eq. (65) are of second order in the coupling constant J and proportional to $\langle S^z_L\rangle\langle S^z_R\rangle$. The difference between this approximation and the perturbation result, where we used Eq. (51) instead of Eq. (71), lies in the assumption of very large ferromagnets, $-i\tilde{\xi}^r_p\approx1$, and thick barriers, $r^r_{\mathcal{P}}\approx1$. The three-dimensional case at zero temperature follows in analogy to Eq. (42).

VII. NUMERICAL RESULTS

In order to make quantitative predictions for comparison with possible experiments, we implement our calculations with model parameters for the geometry of the trilayer junction similar to those studied by Moodera *et al.*[8] and for simplicity take the same ferromagnetic materials on either side of the barrier. The parameters for Ni and Fe are taken from Mukasa *et al.*[49] in order to obtain a rough estimate for the conduction-band splitting. The values are collected in Table

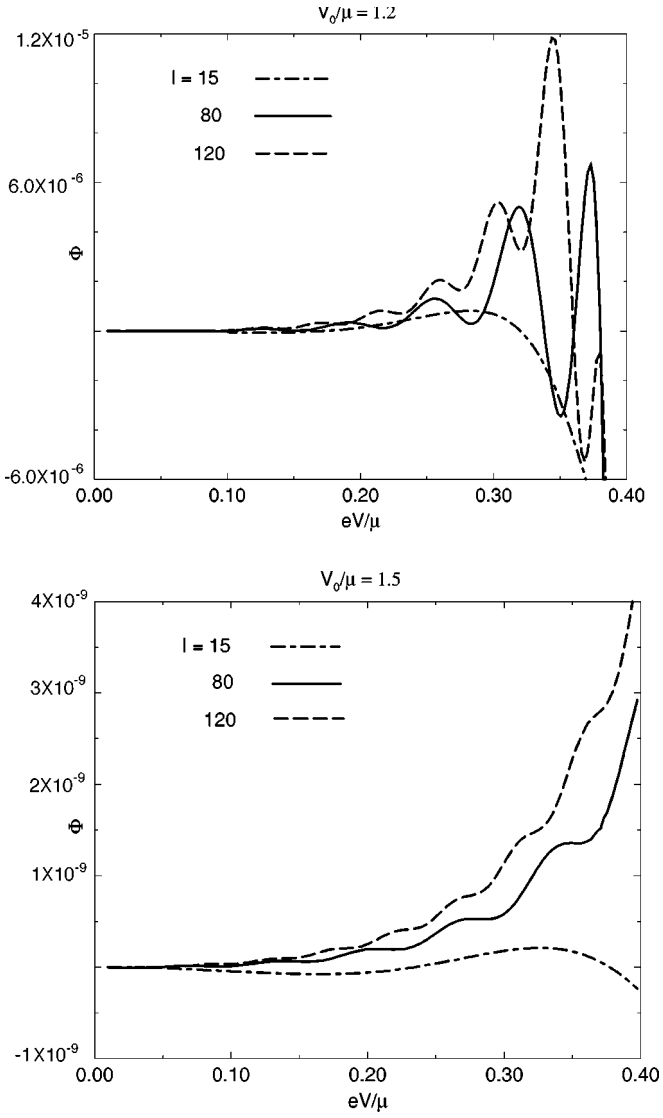

FIG. 2. Range function Φ in the perturbation model vs applied bias across the junction for different ferromagnetic slab thicknesses $l=15$, 80, 120 Å . The barrier thickness is assumed $s=12$ Å and the ratio of barrier height to Fermi energy $V_0/\mu=1.2$ for MgO and $V_0/\mu=1.5$ for Al_2O_3, respectively.

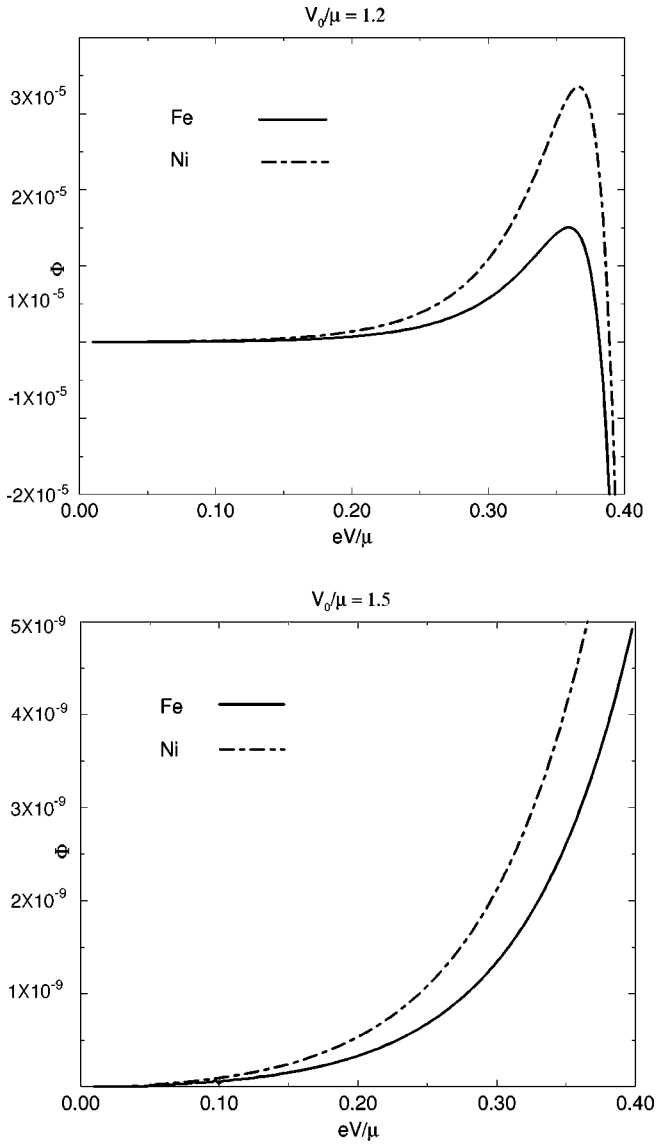

FIG. 3. Range function Φ in the mean-field model vs applied bias across the junction for different ferromagnetic materials Fe, Ni with slab thicknesses $l=15$ Å . The barrier thickness is assumed $s=12$ Å and the ratio of barrier height to Fermi energy $V_0/\mu=1.2$ for MgO and $V_0/\mu=1.5$ for Al_2O_3, respectively.

I, where the value for the Fermi wave vector in equilibrium k_F implies an effective electron mass of $m/m_e=1.20$. We always take the zero-temperature limit and, according to our model in Fig. 1, express the barrier Green's functions in terms of Airy functions (cf. Appendix D).

It is convenient to define the dimensionless interaction range function, which represents the variation of the interaction between ferromagnetic slabs, in the form

$$\Phi(l)=-\left(\frac{\pi\hbar}{\mu_0}\right)^2\frac{\pi E_{\mathrm{ex}}^{3\mathrm{D}}(l)}{h_0^L h_0^R\, m\, \nu^{2\mathrm{D}}}. \tag{72}$$

This depends on the width of the slabs, which for simplicity is assumed to be the same for both $l=l_L=l_R$, on the form of the barrier and also on the bias. The change in the coupling behavior of the ferromagnets is shown as a function of applied bias eV/μ for the perturbation model, Fig. 2, and mean-field model, Fig. 3, respectively. For both models the range function is calculated for barriers with thickness $s=\mathcal{R}-\mathcal{L}=12$ Å for two different barrier materials, MgO and Al_2O_3, i.e., for two different initial ratios of the barrier height to the equilibrium Fermi energy $V_0/\mu=1.2$ and $V_0/\mu=1.5$, respectively. Additionally, we varied the length of the ferromagnets between a very thin slab $l=15$ Å and what was achieved in recent experiments by vacuum evaporation[8] or sputtering techniques[10] $l=80$, 120 Å .

In Fig. 2 the range function shows oscillatory behavior as the bias is varied. For very thin barrier thickness $l=15$ Å the period of the oscillations is very long and, in the range plotted, exhibits only one full oscillation whose amplitude grows stronger and period shorter as the bias is turned up. For the two different barrier materials the oscillations show similar qualitative but different detailed behavior. This is mainly due to a stronger exponential damping for the higher barrier that reduces not only the coupling strength but also the relative

strength of the oscillations. The proportional increase of oscillation strength with increase of bias can be understood from the fact that for greater bias the spin current becomes stronger so that the interaction between the slabs is largely influenced by the effect of the spin current according to Eq. (65). Furthermore, the decrease of the oscillation period is also connected to the spin current. The two cutoffs of the frequency integration in Eq. (61) lead approximately to a wave vector $q_{eV}=\sqrt{2m\,eV}/\hbar$, since $V^L-V^R=eV$, which contains the bias implicitly. This wave vector is responsible for the principal oscillation out of equilibrium. For a detailed discussion we refer to Ref. 38. The oscillations that do not vanish in equilibrium are considerably weaker and are not visible on the scale used in the figures.

Increasing the thickness of the ferromagnetic slabs, we find for MgO that the behavior described above becomes more pronounced for $l=80$ Å beyond which two types of oscillations start to occur, i.e., for $l=120$ Å: a strong ''slow'' oscillation and a weaker ''fast'' one. For Al_2O_3 the separation into slow and fast oscillations is already visible at $l=80$ Å. The fast oscillations grow more rapid for both MgO and Al_2O_3 since the exchange interaction is a function of the slab length l. Further, the faster the oscillations the stronger their destructive interference so that in the Al_2O_3 barrier they appear to be very strongly damped and for $l=120$ Å have almost vanished completely. Finally, the strength of the slow oscillations increases for larger l, since in Eq. (61) the term $\tilde{\xi}_0$ is proportional to l, which is another indication that the term proportional to the spin current indeed dominates the nonequilibrium exchange interaction. To explain them in more detail, we point out that for Al_2O_3 and $l=120$ Å the parameters lie within the range of the mean-field model where we can assume that semi-infinite slabs are a good approximation of the ferromagnets in the junction.

Thus, we turn to Fig. 3 and find that here the fast oscillations disappeared and the curves can be roughly viewed as envelopes to those in the perturbation model. However, there are two fundamental differences. Since Ni and Fe have different band splitting, the transmission through the barrier is altered for the different materials, leading to stronger coupling for Fe whose mean field is approximately twice as strong as that of Ni. Further, here the coupling strength for the barrier thickness $l=15$ Å is already as strong as for $l=120$ Å in the perturbation model. The reason is that in calculating the exchange in the mean-field model (68) we assumed that one of the slabs was semi-infinite and that the interaction was taken into account to all orders, because in the unperturbed Hamiltonian (2) we replaced the single particle potential $V(x)$ (3) by the spin-dependent potential $V_\alpha(x)$ (8).

What is common to both models is the general behavior of the interaction switching from a ferromagnetic coupling to an antiferromagnetic one at an applied voltage of $\sim 0.38eV/\mu$ in the case of the MgO barrier. This switching behavior is absent for the higher Al_2O_3 barrier at this bias. Without showing a graph, we note that a switching nevertheless occurs at much higher bias of $\sim 0.8eV/\mu$. In a sense the behavior of the Al_2O_3 barrier shows the same general coupling behavior as the lower MgO one; only it is, first, much stronger damped and, second, its general features vary over a wider range of applied voltages.

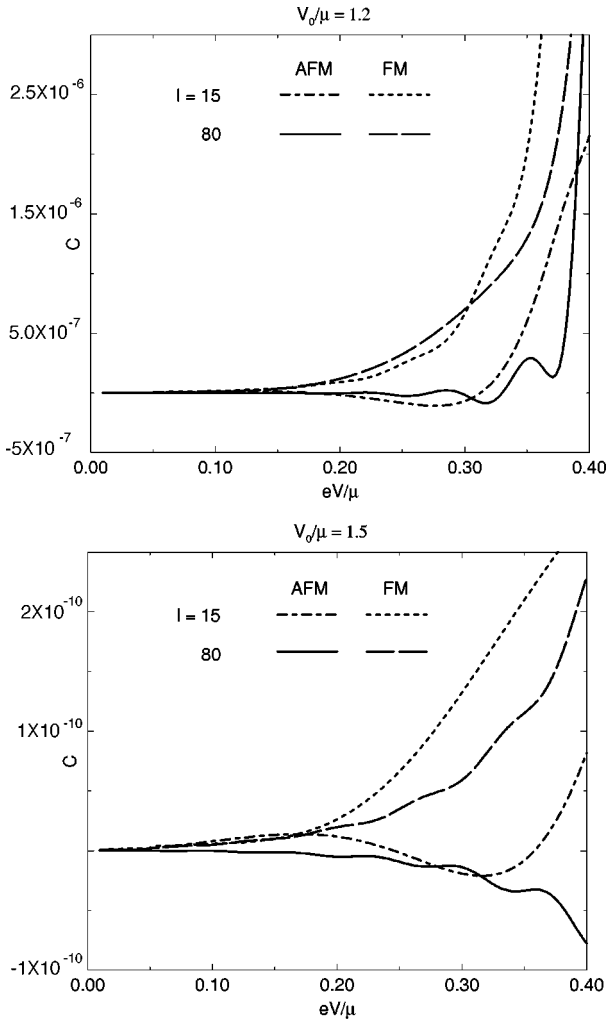

FIG. 4. Normalized spin current-voltage function $C[A]$ in the perturbation model for parallel [ferromagnetic (FM)] and antiparallel [antiferromagnetic (AFM)] alignment of the ferromagnets. The thicknesses of the ferromagnets are $l=15$ and 80 Å and of the barrier $s=12$ Å. The ratio of barrier height to Fermi energy are $V_0/\mu=1.2$ for MgO and $V_0/\mu=1.5$ for Al_2O_3, respectively.

In reference to the analytical results discussed in Sec. VI A, we would like to demonstrate how the switching is reflected in the spin current. We turn to Fig. 4, where we introduced the normalized function

$$C(l)=-\frac{(2\pi\hbar)^2}{2m\,\mu_0 h_0 \nu^{2D}}\langle \mathcal{I}_{spt}^{\mathrm{3D,\,Per}}\rangle, \tag{73}$$

which has the dimension $[A]$, and assumed $h_0=|h_0^L|=|h_0^R|$ and $l=l_L=l_R$. Figure 4 shows the spin-current-voltage behavior for ferromagnetic and antiferromagnetic alignment of the slabs. As in the case of the exchange interaction, the length of the ferromagnets is varied between $l=15$ Å and $l=120$ Å. The barrier again is $l=12$ Å wide and consists of either MgO or Al_2O_3.

The switching from parallel to antiparallel alignment in the exchange interaction reappears at a slightly lower bias in the form of switching of the spin current from a negative to a positive spin current in the antiferromagnetic set up of the junction. For slabs $l=15$ Å exists a switching for both barrier materials, whereas for slabs $l=80$ Å the switching occurs only for the MgO barrier, similar to the exchange interaction in Fig. 2. This demonstrates the proportionality between exchange interaction and spin current in the antiferromagnetic configuration of the junction as pointed out in Sec. VI A. In real systems other contributions such as the various anisotropy energies have to be included where in most experiments the tunnel magnetoresistance is controlled by an external magnetic field. A quantitative estimate with an account of these additional contributions will be given in a subsequent publication.

Looking at both graphs, we observe that oscillations primarily show in the antiparallel ordered structure whereas for the parallel one they are almost completely damped. To explain this behavior, we examine Eq. (46). The two spin contributions $\langle \mathcal{I}_{spt,L(R)} \rangle$, are different in their behavior. The contribution to the spin current arising from the left of the barrier $\langle \mathcal{I}_{spt,L} \rangle$ comes from the region of higher chemical potential μ. Therefore, $\langle \mathcal{I}_{spt,L} \rangle$ predominantly shows characteristic tunneling behavior where oscillations are strongly damped. On the other hand, in the right region of lower chemical potential $\mu - eV$ the spin current mainly flows into the right reservoir away from the junction so that there is a higher sensitivity to interferences in $\langle \mathcal{I}_{spt,R} \rangle$, arising from scattering of localized spins and reflection of the barrier. If the two contributions are added, as it is the case for a ferromagnetically aligned structure, the oscillations are relatively small compared to the overall spin current. On the contrary, if the two contributions are subtracted, as is the case for an antiferromagnetically aligned structure, the oscillations can become large relative to the overall spin current.

VIII. DISCUSSION

Some comparison is possible between the results derived for a simple model in the previous section and recent experiments on tunneling in ferromagnet-insulator-ferromagnet trilayer thin-film planar junctions. Most experimental measurements in trilayer junctions are concerned with the change in resistance as a function of an applied external magnetic field. According to a model by Julliere,[4] it is argued that due to an uneven spin distribution of conduction electrons in the ferromagnets the probability of tunneling through the insulator depends on the relative orientation of the ferromagnets. In the parallel configuration, there is a maximum match between the number of the occupied states in one lead and available states in the other, giving a maximum in the tunnel current and a minimum in the tunnel resistance. On the other hand, in the antiparallel configuration, tunneling is between majority states in the one lead and minority states in the other that leads to the inverse of this behavior. This argument holds as long as the barriers are relatively high and thick and the ferromagnetic slabs long so that the conditions for Eq. (71) hold. Numerous experiments have validated that this model roughly predicts the behavior of the measured magnetoresistance curves. Further, Slonczewski[13] pointed out that the interlayer exchange coupling in a trilayer junction can become negative, depending on the barrier height of the insulating potential. In magnetoresistance curves for Ni $-$ Fe/Al_2O_3/Co junctions Miyazaki *et al.* found an additional step that they related to a negative interlayer exchange coupling, i.e., an antiferromagnetic one.[50] They stressed that the coupling also depends on the junction area. If the junction is not too small, edge effects can be neglected so that our three-dimensional expressions for the coupling and spin current give a proper account of the effect of the junction area on the coupling strength.

One of the most surprising experimental observations concerns the strong decrease of magnetoresistivity as the bias is increased. Moodera *et al.* reported for their junctions that the change in magnetoresistance is small for dc biases up to $0.1V$ beyond which it decreased much faster.[8] In addition, MgO barriers showed more decrease as compared to Al_2O_3 barriers. Finally, the decrease of the magnetoresistance with bias was larger when the magnetoresistance at low bias was smaller. Although the behavior might be different on a detailed level, our model incorporates qualitatively all the phenomena described above. Turning once again to Figs. 2 and 3 describing the interlayer exchange coupling, we find that the initial region is rather flat thereafter the influence of the bias is strongly increased. In particular, strong nonlinear current-voltage behavior occurs at lower bias, if the barrier height and the Pauli factor, i.e., the band splitting, are smaller, in correspondence to the experimental results. Further, in agreement with the experiments by Parkin *et al*. on metallic superlattices,[24] where the oscillations in the magnetoresistance could be related to the oscillations in the exchange coupling by measuring the saturation field, we find that a voltage-induced rise in the ferromagnetic coupling strength is related to a decrease in the tunnel magnetoresistance. Detailed calculations of the strength and nonlinearity of the increase of the ferromagnetic coupling appear to be compatible with the significant decrease of magnetoresistance observed. This work will be reported in detail elsewhere.

IX. CONCLUSION

In this paper, we have studied tunneling in ferromagnet-insulator-ferromagnet thin-film planar junctions out of equilibrium. Using a proper field theoretic description for such a system, which is based on the nonequilibrium Keldysh formalism, it was possible to extend previous treatments of the spin current and exchange interaction. In particular, we derived a Landauer-type formula for both our models and could explain the spin-coupled interface resistance, first discussed by Johnson and Silsbee[15,16,51] and further developed by Valet and Fert.[52] Because our models describe coherent transport, the spin accumulation occurs throughout each ferromagnet, only depending on the barrier properties, the differences in the chemical potentials in the two reservoirs, and, in case of the perturbation model, on the thicknesses of the ferromagnets.

Terms in the nonequilibrium exchange interaction, which are proportional to the length of the ferromagnetic slabs,

were related to spin currents arising from an *s-d* interaction in each slab. This leads to an approximate, physically intuitive formula for the nonconvergent behavior of the exchange interaction out of equilibrium for $l_p \to \infty$, i.e., this contribution to the interaction appears to act as an uniform magnetic field. In addition, the numerical results show an interesting switching behavior between parallel and antiparallel coupling between the slabs for different applied biases under feasible experimental conditions. In particular, this leads to an explanation of the strong decrease of the tunnel magnetoresistance observed with increasing bias.

By using two different models, the mean-field model and perturbation model, different aspects of the trilayer junction were captured and shown to be related, i.e., the perturbation treatment is the natural approach for calculating the exchange interaction as it has been done for the RKKY interaction, whereas the mean-field approach is the more obvious one for treating the spin-polarized current. Under certain limiting conditions these two models lead to the same results. Naturally, it seems desirable to unify both models in a way that there is a possibility of treating strong coupling constants for finite ferromagnets. This can be done within the mean-field model, if the assumptions of semi-infinite ferromagnets is dropped and the potential structure is extended to cover the full ferromagnet-barrier-ferromagnet trilayer junction in the intermediate region instead.

To obtain a better quantitative picture of tunneling in a trilayer structure, one would like to include effects such as barrier nonuniformity, spin-flip processes, and carrier-carrier and carrier-magnon interactions. Although our elementary trilayer model omits these generally important complications, we believe that the nonequilibrium Green's function method is adaptable to include them. For example, the barrier nonuniformity could be treated within a coherent potential approximation to the lateral modulation of the barrier thickness between the ferromagnets and the insulator. Of particular importance are also the effects caused by spin excitations. In this context we note the recent work by Zhang *et al.*[53] who could explain the quenching of magnetoresistance for the zero bias anomaly observed by Julliere. It would be interesting to extend the treatment of spin excitations to the nonequilibrium case. Another aspect we are investigating at present are the spin-wave dynamics of the junctions as pointed out by Zilberman.[54]

ACKNOWLEDGMENTS

We would like to thank Dr. N. F. Schwabe for making useful suggestions. R.J.E. wishes to acknowledge the support provided by the Leverhulme Foundation.

APPENDIX A: COMPARISON TO TRANSFER MATRIX

To make a closer connection between scattering theory and the nonequilibrium Green's function approach, it is useful to derive relations between Green's functions and the scattering or transfer matrix. A significant aspect of the scattering theory is that it allows for a separation between the initial conditions, which can be adapted to the requirement of any particular problem, and a scattering or transfer matrix that depends only on the nature of the dynamics, the forces, and the frequency. Since all aspects in this section only deal with single electron quantities, we drop the spin index for clarity.

The scattering formalism describes the electrons in terms of in- and out-scattering states of the conductor that are related by the scattering matrix

$$\begin{pmatrix} a_{out} \\ b_{out} \end{pmatrix} = \mathbf{S} \begin{pmatrix} a_{in} \\ b_{in} \end{pmatrix}, \tag{A1}$$

where **S** is a unitary matrix due to current conservation that has the block structure

$$\mathbf{S} = \begin{pmatrix} s_{LL} & s_{LR} \\ s_{RL} & s_{RR} \end{pmatrix}. \tag{A2}$$

Another equivalent description is via the transfer matrix. The scattering and transfer matrices are equivalent descriptions for transmission through the intermediate, disordered region of the system. A convenient property of the transfer matrix is the multiplicative composition rule: the transfer matrix of a number of disordered regions in series separated by ideal leads is the product of the individual transfer matrices. The scattering matrix, in contrast, has a more complicated composition rule.

To be more explicit consider again the local, single-particle potential $V(x)$ in H_0 (2). The potential is continuous and it is assumed that the fundamental set of solutions of the Schrödinger equation in the appropriate subspace $\{v_1^p(x), v_2^p(x)\}$, $p \in \{L, I, R\}$ is known. Therefore, the transfer matrix for transporting the wave function consists of a linear combination of eigenfunctions with appropriate coefficients a_p, b_p, and their derivatives in the interval $[\mathcal{L}, \mathcal{R}]$. A free wave $v_1^L(x) = \exp(iq_L x)$ incident from the left is scattered off the potential and partly transmitted to the right, $v_1^R(x) = \exp(iq_R x)$, which leads to the following equation for the transfer matrix:

$$\begin{pmatrix} a_R \\ b_R \end{pmatrix} = \mathbf{T} \begin{pmatrix} a_L \\ b_L \end{pmatrix}, \tag{A3}$$

where we identify $a_L = a_{in}$, $b_L = a_{out}$, $a_R = b_{out}$, $b_R = b_{in}$, and

$$\mathbf{T}=\begin{pmatrix} v_1^R(\mathcal{R}) & v_2^R(\mathcal{R}) \\ v_1'^R(\mathcal{R}) & v_2'^R(\mathcal{R}) \end{pmatrix}^{-1}\begin{pmatrix} v_1^I(\mathcal{R}) & v_2^I(\mathcal{R}) \\ v_1'^I(\mathcal{R}) & v_2'^I(\mathcal{R}) \end{pmatrix}\begin{pmatrix} v_1^I(\mathcal{L}) & v_2^I(\mathcal{L}) \\ v_1'^I(\mathcal{R}) & v_2'^I(\mathcal{L}) \end{pmatrix}^{-1}\begin{pmatrix} v_1^L(\mathcal{L}) & v_2^L(\mathcal{L}) \\ v_1'^L(\mathcal{L}) & v_2'^L(\mathcal{L}) \end{pmatrix}$$
$$\equiv -\frac{1}{2i\sqrt{q_Rq_L}W}\begin{pmatrix} -iq_Re^{-iq_R\mathcal{R}} & -e^{-iq_R\mathcal{R}} \\ -iq_Re^{iq_R\mathcal{R}} & e^{iq_R\mathcal{R}} \end{pmatrix}\begin{pmatrix} \Gamma_L & -\Lambda \\ \Omega & \Gamma_R \end{pmatrix}\begin{pmatrix} e^{iq_L\mathcal{L}} & e^{-iq_L\mathcal{L}} \\ iq_Le^{iq_L\mathcal{L}} & -iq_Le^{-iq_L\mathcal{L}} \end{pmatrix}.$$

The conservation of probability density in stationary state implies that $\det\mathbf{T}=1$. From the transmission matrix the transmission coefficient through the system can be calculated:

$$T(\omega)=\frac{|a_R|^2}{|a_L|^2}=\frac{1}{|T_{22}|^2}=\frac{4W^2q_Lq_R}{(\Omega+q_Lq_R\Lambda)^2+(q_L\Gamma_R+q_R\Gamma_L)^2}. \tag{A4}$$

The transfer matrix, on the other hand, can also be written in terms of Green's functions

$$\mathbf{T}=-\frac{1}{2i\sqrt{q_Rq_L}W}\begin{pmatrix} D^r\Lambda e^{i(q_L\mathcal{L}-q_R\mathcal{R})} & -D^a\Lambda[1-i\hbar v_RG^r(\mathcal{R},R)]e^{-i(q_L\mathcal{L}+q_R\mathcal{R})} \\ D^a\Lambda[1-i\hbar v_LG^r(\mathcal{L},L)]e^{i(q_L\mathcal{L}+q_R\mathcal{R})} & -D^a\Lambda e^{-i(q_L\mathcal{L}-q_R\mathcal{R})} \end{pmatrix}.$$

Therefore, the product $\hbar^2G^a(\mathcal{L},\mathcal{R})G^r(\mathcal{R},\mathcal{L})v_Lv_R$ amounts to

$$\hbar^2G^a(\mathcal{L},\mathcal{R})G^r(\mathcal{R},\mathcal{L})v_Lv_R=\frac{4q_Lq_R}{|D|^2}\gamma_I^a(\mathcal{L},\mathcal{R})\gamma_I^r(\mathcal{R},\mathcal{L})=\frac{4W^2q_Lq_R}{(\Omega+q_Lq_R\Lambda)^2+(q_L\Gamma_R+q_R\Gamma_L)^2}, \tag{A5}$$

which equals $T(\omega)$ (see also Ref. 55). Further, there exists a one-to-one relation between the transfer matrix and the scattering matrix

$$\mathbf{S}=\begin{pmatrix} -T_{21}/T_{22} & 1/T_{22} \\ -1/T_{22} & -T_{12}/T_{22} \end{pmatrix}, \tag{A6}$$

with which a relation between the scattering matrix and the Green's functions of the system can be established,

$$\mathbf{S}=\begin{pmatrix} [1-i\hbar v_LG^r(\mathcal{L},\mathcal{L})]e^{2iq_L\mathcal{L}} & -i\hbar\sqrt{v_Lv_R}G^r(\mathcal{R},\mathcal{L})e^{i(q_L\mathcal{L}-q_R\mathcal{R})} \\ -i\hbar\sqrt{v_Lv_R}G^r(\mathcal{R},\mathcal{L})e^{i(q_L\mathcal{L}-q_R\mathcal{R})} & [1-i\hbar v_RG^r(\mathcal{R},\mathcal{R})]e^{-2iq_R\mathcal{R}} \end{pmatrix}.$$

The diagonal elements of the scattering matrix describe reflection off the respective interface, whereas the off-diagonal elements are the transmission through the system. The elements of the scattering matrix amplitude can thus written in the compact notation[55]

$$s_{pq}^r=\delta_{pq}-i\hbar\sqrt{v_pv_q}G_\alpha^r(\mathcal{P},\mathcal{Q}), \tag{A7}$$

where $p,q\in\{L,R\}$ and $\mathcal{P},\mathcal{Q}\in\{\mathcal{L},\mathcal{R}\}$. Therefore, the reflection amplitudes at the interfaces are given by $r_{\mathcal{P}}^r\equiv s_{pp}^r$ and the transmission amplitude through the intermediate region by $t^r\equiv s_{LR}^r$.

APPENDIX B: SPECTRAL RELATIONS

The following identity can intuitively be seen in direct connection to the spectral relation:

$$G^a(\mathcal{P},\mathcal{Q})-G^r(\mathcal{P},\mathcal{Q})=A_L(\mathcal{P},\mathcal{Q})+A_R(\mathcal{P},\mathcal{Q}), \tag{B1}$$

where $\{\mathcal{P},\mathcal{Q}\}\in\{\mathcal{L},\mathcal{R}\}$. The proof given in Ref. 42 allows for the reasoning that the fully coupled system in nonequilibrium steady state only depends on the occupation properties of the reservoirs in the asymptotic regions of the left and right leads. This behavior shows in a mathematical form in the functional relations $(\Gamma_L\Gamma_R-W^2)\delta(\Lambda)=0$ and $\Lambda\delta(\Lambda)=0$, for example. They prove the fact that the imaginary parts of Green's functions in the intermediate region γ_I cancel.[42] This restates that there is no dependence on the occupation of the intermediate region.

APPENDIX C: GREEN'S FUNCTIONS OF THE LEAD AND SPATIAL INTEGRATION

Within the single effective mass approximation for a barrier system as shown in Fig. 1 the Green's functions of the decoupled leads are found to be

$$g_{L(R),\alpha}^{r/a}(x,x')=+(-)\frac{2m}{\hbar^2q_{L(R),\alpha}^{r/a}}\begin{cases} \sin\{q_{L(R),\alpha}^{r/a}[x-L(R)]\}e^{\mp(\pm)iq_{L(R),\alpha}^{r/a}[x'-L(R)]}, & x>(<)x' \\ \sin\{q_{L(R),\alpha}^{r/a}[x'-L(R)]\}e^{\mp(\pm)iq_{L(R),\alpha}^{r/a}[x-L(R)]}, & x'>(<)x, \end{cases} \tag{C1}$$

where $q^{r/a}_{L(R),\alpha}=\sqrt{2m(\hbar\omega-V^{L(R)}_{\alpha}\pm i\delta)/\hbar^2}$, the upper/lower signs are associated with the superscripts r/a, respectively, and $V^{L(R)}_{\alpha}$ is the bottom of the conduction band in the corresponding side of the junction as before. Furthermore, the explicit frequency and wave-vector dependence was omitted for brevity. Thus, from Eq. (C1) follows

$$\chi^{r/a}_{L(R),\alpha}(\mathcal{L}(\mathcal{R}),x_{L(R)})=\chi^{r/a}_{L(R),\alpha}[x_{L(R)},\mathcal{L}(\mathcal{R})]=+(-)\exp\{\mp(\pm)iq^{r/a}_{L(R),\alpha}[x_{L(R)}-\mathcal{L}(\mathcal{R})]\}. \tag{C2}$$

The spatial integrations yield

$$\tilde{\xi}^{r/a}_{L(R),\alpha}=2q^{r/a}_{L(R),\alpha}\int_{L-l_L}^{L}\left(\int_{R}^{R+l_R}\right)dx_{L(R)}\,\tilde{\chi}^{r/a}_{L(R)}=\mp i[\exp(\pm 2iq^{r/a}_{L(R),\alpha}l_{L(R)})-1], \tag{C3}$$

and

$$\xi^{0}_{L(R)}=\int_{\mathcal{L}-l_L}^{\mathcal{L}}\left(\int_{\mathcal{R}}^{\mathcal{R}+l_R}\right)dx_{L(R)}\,\chi^{r}_{L(R)}[x_{L(R)},\mathcal{L}(\mathcal{R})]\chi^{a}_{L(R)}[\mathcal{L}(\mathcal{R}),x_{L(R)}]=\frac{\exp[i(q^{r}_{L(R),\alpha}-q^{a}_{L(R),\alpha})l_{L(R)}]-1}{i(q^{r}_{L(R),\alpha}-q^{a}_{L(R),\alpha})}, \tag{C4}$$

where $\xi^{0}_{L(R)}$ produces a term of $l_{L(R)}$ for energies above the band bottom in the respective lead, i.e., $\hbar\omega\geqslant V^{L(R)}$.

APPENDIX D: GREEN'S FUNCTIONS FOR THE SLOPING BARRIER

A sloping potential leads to the following inhomogeneous Schrödinger equation in

$$[\partial_x^2-\kappa^3 x]f(x)=\zeta, \tag{D1}$$

with the parameters $\kappa=-\sqrt[3]{2\mathrm{meV}/[\hbar^2(\mathcal{R}-\mathcal{L})]}$ and $\zeta=2m(V_0-eV/2-\omega)/\hbar^2$. Two independent solutions are found in terms of Airy functions,[56]

$$v_1(x)=\mathrm{Ai}(\kappa x+\zeta/\eta^2),$$

$$v_2(x)=\mathrm{Bi}(\kappa x+\zeta/\eta^2). \tag{D2}$$

The Green's function g_I for the sloping barrier is then obtained by inserting v_1 and v_2 into

$$g_I(x,x')=\frac{2m}{\hbar^2}\frac{1}{W\Lambda}\begin{cases}Q(x)K(x'), & x>x'\\ K(x)Q(x'), & x<x',\end{cases} \tag{D3}$$

where

$$Q(x)=v_1(x)v_2(\mathcal{R})-v_2(x)v_1(\mathcal{R}),$$

$$K(x)=v_1(x)v_2(\mathcal{L})-v_2(x)v_1(\mathcal{L}),$$

$$\Lambda=v_1(\mathcal{L})v_2(\mathcal{R})-v_2(\mathcal{L})v_1(\mathcal{R}),$$

and $W=v_1v_2'-v_2v_1'$ the Wronskian. In equilibrium, one can show that $g_I(x,x')$ simplifies to

$$g_I(x,x')=\frac{2m}{\hbar^2}\begin{cases}\dfrac{\sinh[k(x-\mathcal{L})]\sinh[k(x'-\mathcal{R})]}{k\sinh[k(\mathcal{R}-\mathcal{L})]}, & x<x'\\ \dfrac{\sinh[k(x'-\mathcal{L})]\sinh[k(x-\mathcal{R})]}{k\sinh[k(\mathcal{R}-\mathcal{L})]}, & x'>x,\end{cases} \tag{D4}$$

where $k=\sqrt{2m(V_0-\hbar\omega)}/\hbar$. Note that Eq. (D4) holds for all ω, i.e., including the case when $V_0-\omega<0$, for which the sinh functions in Eq. (D4) go over to corresponding sin functions.

[1] P. Grünberg, R. Schreiber, Y. Pang, M. B. Brodsky, and H. Sowers, Phys. Rev. Lett. **57**, 2442 (1986).

[2] P. M. Levy, in *Solid State Physics*, edited by H. Ehrenreich and D. Turnbull (Academic, New York, 1994), Vol. 47.

[3] J. M. Daughton, Thin Solid Films **216**, 162 (1992).

[4] M. Julliere, Phys. Lett. **54A**, 225 (1975).

[5] S. Maekawa and U. Gäfvert, IEEE Trans. Magn. **18**, 707 (1982).

[6] Y. Suezawa, F. Takahashi, and Y. Gondo, Jpn. J. Appl. Phys., Part 2 **31**, L1415 (1992).

[7] J. Nowak and J. Rauluszkiewicz, J. Magn. Magn. Mater. **109**, 79 (1992).

[8] J. S. Moodera and L. R. Kinder, J. Appl. Phys. **79**, 4724 (1996).

[9] T. Miyazaki and N. Tezuka, J. Magn. Magn. Mater. **139**, L231 (1995).
[10] W. J. Gallagher, S. S. P. Parkin, Yu Lu, X. P. Bian, A. Marley, K. P. Roche, R. A. Altman, S. A. Rishton, C. Jahnes, T. M. Shaw, and Gang Xiao, J. Appl. Phys. **81**, 3741 (1997).
[11] J. M. Daughton, J. Appl. Phys. **81**, 3758 (1997).
[12] P. M. Tedrow and R. Meservey, Phys. Rev. Lett. **26**, 192 (1971).
[13] J. C. Slonczewki, Phys. Rev. B **39**, 6995 (1989).
[14] A. G. Aronov, Pis'ma Zh. Éksp. Teor. Fiz. **24**, 37 (1976) [JETP Lett. **24**, 32 (1976)].
[15] Mark Johnson and R. H. Silsbee, Phys. Rev. Lett. **55**, 1790 (1985).
[16] Mark Johnson and R. H. Silsbee, Phys. Rev. B **37**, 5312 (1988).
[17] C. Caroli, R. Combescot, P. Noziéres, and D. Saint-James, J. Phys. C **4**, 916 (1971).
[18] C. Caroli, R. Combescot, P. Noziéres, D. Lederer, and D. Saint-James, J. Phys. C **4**, 2598 (1971).
[19] R. Combescot, J. Phys. C **4**, 2611 (1971).
[20] C. Caroli, R. Combescot, P. Noziéres, and D. Saint-James, J. Phys. C **5**, 21 (1972).
[21] T. E. Feuchtwang, Phys. Rev. B **10**, 4121 (1974).
[22] T. E. Feuchtwang, Phys. Rev. B **10**, 4135 (1974).
[23] T. E. Feuchtwang, Phys. Rev. B **13**, 517 (1976).
[24] S. S. P. Parkin, N. More, and K. P. Roche, Phys. Rev. Lett. **64**, 2304 (1990).
[25] Y. Yafet, Phys. Rev. B **36**, 3948 (1987).
[26] W. Baltensperger and J. S. Helman, Appl. Phys. Lett. **57**, 2954 (1990).
[27] P. Bruno and C. Chappert, Phys. Rev. Lett. **67**, 1602 (1991).
[28] D. M. Edwards, J. Mathon, R. B. Muniz, and M. S. Phan, Phys. Rev. Lett. **67**, 493 (1991).
[29] D. M. Edwards, J. Mathon, R. B. Muniz, and M. S. Phan, J. Phys.: Condens. Matter **3**, 4941 (1991).
[30] M. D. Stiles, Phys. Rev. B **48**, 7238 (1993).
[31] P. Bruno, Europhys. Lett. **23**, 615 (1993).
[32] J. d'Albuquerque e Castro, J. Mathon, M. Villeret, and D. M. Edwards, Phys. Rev. B **49**, 16 062 (1994).
[33] P. Bruno, Phys. Rev. B **52**, 411 (1995).
[34] P. J. H. Bloemen, M. T. Johnson, M. T. H. van de Vorst, R. Coehoorn, J. J. de Vries, R. Jungblut, J. van de Stegge, A. Reinders, and W. J. M. de Jonge, Phys. Rev. Lett. **72**, 764 (1994).
[35] J. Barnas, J. Magn. Magn. Mater. **111**, L215 (1992).
[36] S. Toscano, B. Briner, H. Hopster, and M. Landolt, J. Magn. Magn. Mater. **114**, L6 (1992).
[37] E. E. Fullerton, J. E. Mattson, S. R. Lee, C. H. Sowers, Y. Y. Huang, G. Felcher, S. D. Bader, and F. T. Parker, J. Magn. Magn. Mater. **117**, L301 (1992).
[38] N. F. Schwabe, N. S. Wingreen, and R. J. Elliott, Phys. Rev. B **54**, 12 953 (1996).
[39] E. Yu. Tsymbal and D. G. Pettifor, J. Phys.: Condens. Matter **9**, L411 (1997).
[40] W. Nolting, A. Vega, and Th. Fauster, Z. Phys. B **96**, 357 (1995).
[41] L. V. Keldysh, Zh. Éksp. Teor. Fiz. **47**, 1515 (1964) [Sov. Phys. JETP **20**, 1018 (1965)].
[42] C. Heide and N. F. Schwabe, Phys. Rev. B **57**, 11 862 (1998).
[43] G. E. W. Bauer, Phys. Rev. Lett. **69**, 1676 (1992).
[44] J. Barnaś and A. Fert, Phys. Rev. B **49**, 12 835 (1994).
[45] P. M. Tedrow and R. Meservey, Phys. Rev. B **7**, 318 (1973).
[46] U. Larsen, Phys. Lett. **85A**, 471 (1981).
[47] J. A. Blackman and R. J. Elliott, J. Phys. C **2**, 1670 (1970).
[48] S. V. Vonsovskii, *Magnetism* (Wiley, New York, 1974).
[49] K. Mukasa, H. Hasegawa, Y. Tazukeand, K. Sueoka, M. Sasaki, and K. Hayakawa, Jpn. J. Appl. Phys., Part 2 **33**, 2692 (1993).
[50] T. Miyazaki, S. Kumagai, and T. Yaoi, J. Appl. Phys. **81**, 3753 (1997).
[51] Mark Johnson and R. H. Silsbee, Phys. Rev. B **35**, 4959 (1987).
[52] T. Valet and A. Fert, Phys. Rev. B **48**, 7099 (1993).
[53] S. Zhang, P. M. Levy, A. C. Marley, and S. S. P. Parkin, Phys. Rev. Lett. **79**, 3744 (1997).
[54] P. E. Zilberman (private communication).
[55] S. Datta, *Electronic Transport in Mesoscopic Systems*, Cambridge Studies in Semiconductor Physics and Microelectronic Engineering Vol. 3 (Cambridge University Press, Cambridge, 1995).
[56] W. Magnus, F. Oberhettinger, and R. P. Soni, *Formulas and Theorems for Special Functions of Mathematical Physics* (Springer-Verlag, Berlin, 1966).